Tectonophysics 833 (2022) 229332

Contents lists available at ScienceDirect

Tectonophysics

journal homepage: www.elsevier.com/locate/tecto

A new interpretation of the metamorphic core in the Taiwan orogen: A regional-scale, left-lateral shear zone that accommodated highly oblique plate convergence in the Plio-Pleistocene

Gong-Ruei Ho [a,*], Timothy B. Byrne [b,c], Jian-Cheng Lee [a], Lucas Mesalles [d], Ching-Weei Lin [e], Wei Lo [f], Chung-Pai Chang [g,h]

[a] Institute of Earth Sciences, Academia Sinica, Taipei, Taiwan
[b] Department of Natural Resources and Environmental Studies, National Dong Hwa University, Hualien, Taiwan
[c] Department of Geosciences, University of Connecticut, Storrs, CT, United States
[d] Department of Earth and Environmental Sciences, National Chung Cheng University, Chiayi, Taiwan
[e] Department of Earth Sciences, National Cheng Kung University, Tainan, Taiwan
[f] Department of Materials and Mineral Resources Engineering, National Taipei University of Technology, Taipei, Taiwan
[g] Department of Earth Sciences National Central University, Zhongli, Taiwan
[h] Center for Space and Remote Sensing Research, National Central University, Zhongli, Taiwan

ARTICLE INFO

Keywords:
Tailuko Belt
Yuli Belt
Slate Belt
Left-lateral shearing
Deformation fabrics
Ductile shear zone
Convergence obliquity

ABSTRACT

In the past decades, the arc-continent collision in Taiwan was commonly interpreted as a relatively continuous process with an invariant plate convergence vector for at least the last 6–5 Ma. This steady convergence, including the rate and the obliquity, between the subducting continental margin and the plate boundary suggest a propagating collision with a space-time equivalence along the developing orogen. More recently, detailed low-temperature geochronologic and plate reconstructions suggest that the plate convergence changed from highly oblique to nearly orthogonal in the last 2 to 1 Ma. This early phase of oblique convergence, driven primarily by the northward motion of the Philippine Sea Plate wrt the Eurasian Plate, implies a significant 'fossil' component of left-lateral, strike-slip motion along the presumably north-trending plate boundary. A synthesis of available data compiled in this study suggests that previously uncharacterized zones of strike-slip deformation exist in the Tailuko Belt, and here we document: 1) the distribution of horizontal shear, 2) the kinematics of deformation, 3) the age of deformation, and 4) regional consistency between geologic studies and plate reconstructions. Horizontal shear may also be recorded at shallow structural levels in southern Taiwan by brittle faults and block rotations. Integration of these new data with previously published kinematic data across strike also suggests plate convergence was partitioned with strike-slip motion in the retrowedge (i.e., the Tailuko Belt) and shortening in the prowedge (i.e., the Slate Belt).

1. Introduction

The island of Taiwan is located at a compressive tectonic boundary between the Eurasian and the Philippine Sea Plates (PSP). The relatively steady-state orogenic process, with about a 7–8 cm/year convergence rate in the NW-SE direction, has been long discussed and provided preliminary ideas for the rock distribution and deformation structures of Taiwan Island in the earlier years (Suppe, 1984; Teng, 1996). More recent plate reconstruction and structural and geochronological studies, however, suggest a relatively complex tectonic history for the convergent boundary (Mesalles et al., 2014; Wu et al., 2016; Zhang et al., 2020; Lee et al., 2015; Hsu et al., 2016). For example, Hsu et al. (2016) and Mesalles et al. (2014) document accelerations in exhumation cooling at 3 and 2 Ma, respectively, which may relate to a change in plate convergence. Wu et al. (2016) also reviewed available paleomagnetic and plate motion data from the PSP and proposed that the convergent vector in the area of Taiwan rotated as much as 50° counterclockwise in the last 2.0 to 1.0 Ma. Although previous plate models (e.g., Hall et al., 1995) argued for an earlier, ~5 Ma, change in motion, Wu et al. included geologic and geochronologic data from southwest Japan

* Corresponding author.
E-mail address: gongruei@earth.sinica.edu.tw (G.-R. Ho).

https://doi.org/10.1016/j.tecto.2022.229332
Received 28 September 2021; Received in revised form 17 February 2022; Accepted 24 March 2022
Available online 12 April 2022

(see e.g., Sibuet et al., 1987; Nakamura et al., 1987; Itoh et al., 1998) that the authors interpreted as evidence of a change in motion of the PSP during 2.0 to 1.0 Ma. More recent geologic and geochronologic data from southwest Japan appear to support the recent change in motion proposed by Wu et al. In particular, geological and geophysical studies of the Median Tectonic Line document a change from thrusting to right-lateral strike-slip faulting at about 0.8 Ma (Mizuno et al., 1999; Sato et al., 2015) and in the forearc seaward of the Median Tectonic Line, Gulick et al. (2010) and Sacks et al. (2013) document a transition from shortening to extension perpendicular to the plate boundary at the time < 1.0 Ma. Although these authors propose that this change reflects subduction zone dynamics, a change in plate kinematics is also possible. In fact, in the eastern part of the forearc, Yamaji (2000) mapped a similar change in fault kinematics and attributed the change to a counterclockwise rotation of the relative motion of the PSP at ~1 Ma. Taken together, these additional observations and the plate reconstruction by Wu et al. (2016) suggest a significant and relatively recent change motion of the PSP relative to Eurasia possibly as young as 1 Ma.

Recent geochronologic and geologic data from Taiwan are consistent with a change in plate motion. Low-temperature geochronologic data from along the length of the Taiwan orogen show "simultaneous" cooling (Mesalles et al., 2014; Lee et al., 2015) since 3 to 2 Ma and possibly as recently as 0.8 Ma (Hsu et al., 2016), which is inconsistent with a propagating collision but supports the 2.0 to 1.0 Ma change in motion proposed by Wu et al. (2016). Geologic studies in the Coastal Range and geophysical studies of the sediments offshore northeastern Taiwan also argue for the initiation of substantial east-west shortening and an increase in erosion of the Backbone Range (i.e., the eastern part of the Central Range) at about 0.8 Ma (Lai et al., 2021; Hsieh et al., 2020). The new plate reconstructions (Wu et al., 2016) therefore suggest highly oblique convergence prior to 2.0 to 1.0 Ma, negating the notion of consistent convergent direction for the Taiwan orogen, and suggesting a significantly different tectonic setting for the orogen.

Previous structural studies in the metamorphic core also suggest significant along-strike material transport at the shallow/middle crust level; although these studies were limited in scope (Faure et al., 1991; Pulver et al., 2002; Clark et al., 1992; Conand et al., 2020) and/or yielded inconsistent senses-of-shear (Faure et al., 1991; Pulver et al., 2002; Mondro et al., 2017; Conand et al., 2020). Here, we build on these early, relatively limited studies with an integrated structural study of a suite of exposures from the most regionally extensive unit in the metamorphic core in the Taiwan orogen, the Tailuko Belt (Fig. 1). Specifically, we report new geologic data from Shoufeng and Wanliqiao Rivers that cross the central part of the Tailuko Belt. These relatively more detailed studies are also complemented with reconnaissance expeditions from 6 additional rivers at different latitudes. These new data suggest a paradigm shift is needed to understand the deformation history of the Taiwan orogen, one that includes significant strike-slip motion at the shallow/middle crust level, and associated ductile deformation preceding the current northwest direction of shortening.

2. Geologic background

Metamorphosed sedimentary rocks mixed with minor but widespread igneous bodies (usually lenticular) makeup over half of the island of Taiwan and crop out between the fold and thrust belt in the west and the colliding arc (Coastal Range) in the east. These metamorphic rocks form two tectonostratigraphic units: a metamorphic core represented by the Tailuko and Yuli Belts and a low-grade metamorphosed sedimentary cover sequence that includes an Eocene to Miocene Slate Belt (Fig. 1). The boundaries between the different cover rocks are interpreted to be gradational. In contrast, an unconformity is interpreted to separate the Cenozoic cover sediments from the Paleo-Mesozoic Tailuko Belt of the metamorphic core. Structurally, all of the metamorphic rocks strike north-northeast except on the both ends of the belt: 1) along a narrow section in southeast Taiwan and 2) in the northern extent of the island where the NW-indentation of the Luzon arc and the opening of the Okinawa Trough have rotated the units clockwise up to 70–80°, forming an orogenic orocline.

2.1. Sedimentary cover sequences

The sedimentary cover can be divided into two, gradational suites that generally differ in age, composition, metamorphic grade, and structural style. The more extensive suite, primarily slates, and metasandstone crops out in the Hsuehshan Range, along the high peaks and western flank of the Backbone Range and as a slice or sliver of rocks in southeast Taiwan that in map view wrap eastward around the southern extent of the Tailuko and Yuli Belts. This more extensive suite ranges in age from Eocene to Miocene and comprises shallow-water shales and basin-fill sandstones with minor interlayers of conglomerate, volcanic rocks (e.g., greenstone, tuffs), and limestone/marble. The suite is interpreted to represent a passive margin sequence formed on southeast Chinese subsiding continental margin. The metamorphic grade of this suite ranges from prehnite – pumpellyite to lower greenschist, and structural deformation styles range from broad, open folds with a steeply dipping axial planar cleavage to isoclinal folds with a dominate, penetrative axial planar cleavage that dips moderately, east-southeast; crenulation cleavages locally developed near the contact with the Tailuko Belt. Because the cleavage is typically well-developed, this suite of metamorphosed cover is locally referred to as the Slate Belt (Yen, 1967; Ho, 1986; Chen and Wang, 1994, 1995), and crops out in both the Hsüehshan and Backbone Ranges.

Although metamorphic grades and structural fabrics are similar, each range is generally characterized by a different kinematics history of strain. For example, in the Hsuehshan Range and western flank of Backbone Range, stretching lineations are down-dip, trending east-southeast; however, strain fringes in the Hsüehshan Range record co-axial strain whereas fringes in the western flank of the Backbone Range record a top-to-the west-northwest sense of shear (Clark et al., 1992; Clark and Fisher, 1995). Tillman and Byrne (1995) interpreted the different deformation histories to be generally contemporaneous with the slate belt: 1) the Hsüehshan Range forming as a popup structure and 2) the western flank Backbone Range representing a regional-scale, top-to-the northwest shear zone. More recently, Ar/Ar dating of synkinematic muscovite and corrensite show deformation associated with cleavage development in the Hsüehshan Range occurred from ~6 to 2 Ma (Chen et al., 2016). Following Tillman and Byrne (1995), we interpret this to be the age of cleavage development in both ranges. This interpretation is consistent with the age of the youngest sediments in the belt (Middle Miocene) and with exhumation cooling ages of reset detrital zircon grains that range from ~5 to ~1.5 Ma (Hsu et al., 2016). Finally, near the contact with the Tailuko Belt, which dips east and the stratigraphy seemingly is overturned, whereas stretching lineations plunge moderately south, and strain fringes record a left-lateral, thrust sense of shear (Clark et al., 1992; Pulver et al., 2002). That is, a component of left-lateral shear is recorded in the easternmost Slate Belt near the contact with the Tailuko Belt.

In southeast Taiwan, where the Slate Belt wraps around the Tailuko and Yuli Belts, the deformation history appears to be more complex (Lu et al., 2001; Chang et al., 2003). In this area, structural fabrics strike east-west to northeast or northwest, strata are strongly folded to be both upright and overturned, and strain fringes associated with an intriguingly low-dipping cleavage record northeast-trending stretching (Conand et al., 2020; Fisher et al., 2002; Mondro et al., 2017). This change in strike, in part, motivated Chang et al. (2003) and Chang et al. (2009) to propose that this area of the slate belt had experienced significant post-cleavage CCW block rotation about a sub-vertical axis, although the associated driving mechanism was unclear.

The second suite of cover rocks crops out almost exclusively in southern Taiwan, primarily on the Hengchun Peninsula. The suite of cover rocks is composed mainly of Miocene sandstone and shale

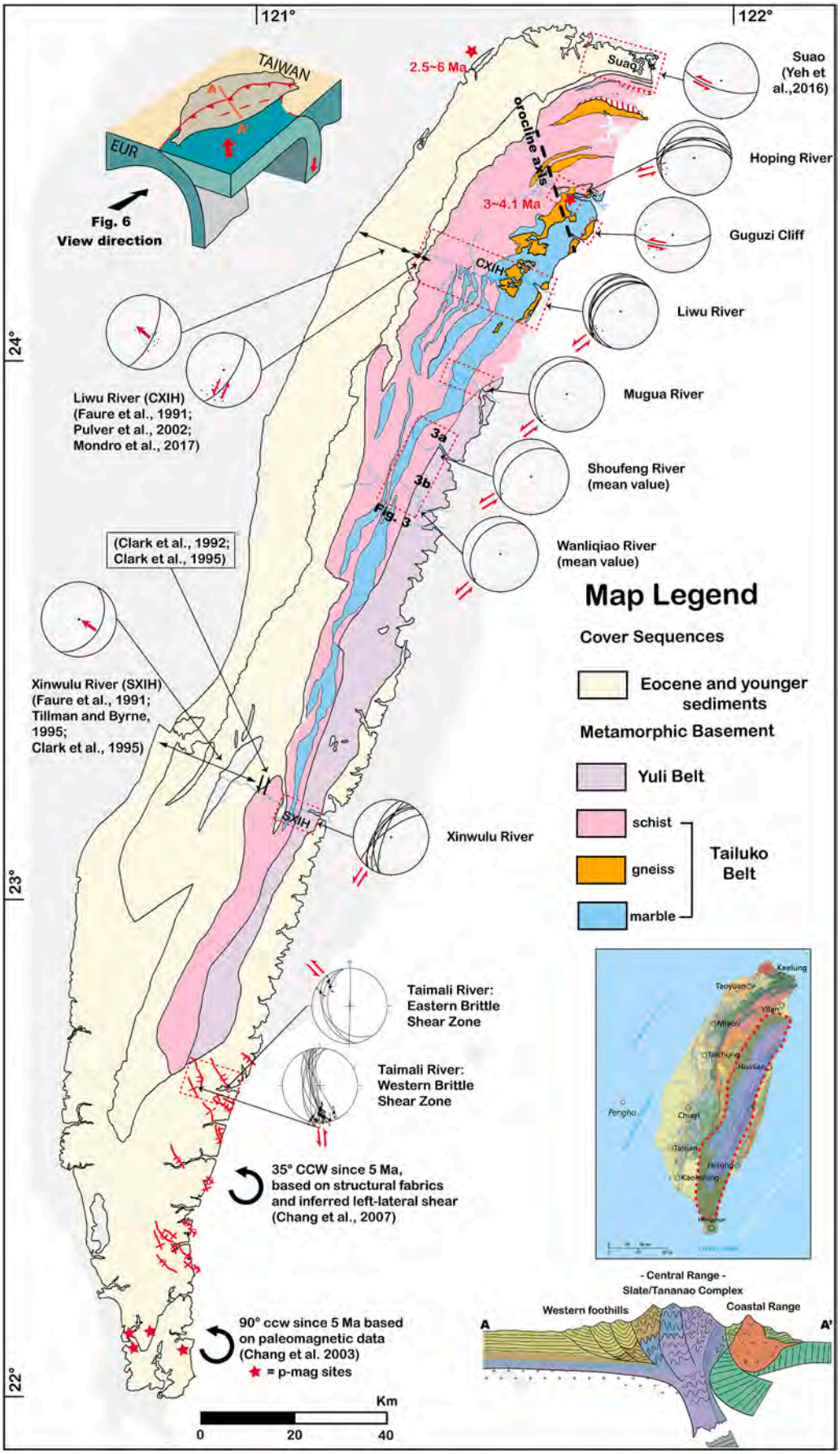

Fig. 1. Geologic map, modified from Central Geologic Survey (2000), and structural data from shear zones in the Tailuko Belt. Stereonets show dominant fabric and associated lineation (interpreted as S2 and L2, respectively) collected or compiled (see text) from areas in red boxes (mostly river or beach transects). Three areas in the north have rotated clockwise due to the opening of the Okinawa Trough (Suppe, 1984). Interpreted block rotations in southern Taiwan are consistent with left-lateral shear interpreted from ductile fabrics, double red arrows. (For interpretation of the references to colour in this figure legend, the reader is referred to the web version of this article.)

sequences that often display many of the characteristics of turbidity current deposits, including graded bedding, sand-filled channel deposits and channel conglomerates (Pelletier and Stephan, 1986; Sung, 1991). The suite is interpreted to represent a relatively deep-water sequence, deposited on either the Chinese passive margin or on oceanic crust of the South China Sea, that was accreted in the early stages of the collision (Chang et al., 2003; Chang et al., 2009). This suite of sediments is only mildly metamorphosed and displays disjunctive cleavage, and less commonly, a penetrative cleavage (Chen and Wang, 1995; Sung, 1991; Chang et al., 2003; Conand et al., 2020). Regional-scale folds trend north-south to east-west (Chang et al., 2009). Paleomagnetic data from 4 sites in the latest Miocene to Pleistocene sequences suggest CCW tectonic rotation about a sub-vertical axis of up to 90° (Fig. 1; Chang et al., 2003).

Mondro et al. (2017) completed a detailed strain study of the dominant cleavage in the sedimentary cover exposed in southeastern Taiwan (i.e., slate belt east of the metamorphic core) and proposed an early history of down-dip stretching followed by strike-parallel stretching. The associated "composite" foliation forms a broad northeast-trending antiform (Fig. 5, Mondro et al., 2017) which is similar to low-dipping S3 foliation recognized in the Tailuko Belt (Stanley et al., 1981; Clark et al., 1992) and to the fabrics along the central cross-island highway (CXIH) that we have re-interpreted as S3 (see below and Pulver et al., 2002). The "composite" stretching direction also trends northeast consistent with the re-interpreted S3 along the CXIH (Fig. 3, Pulver et al., 2002).

2.2. Tailuko Belt

The Tailuko Belt consists of highly deformed interlayers of

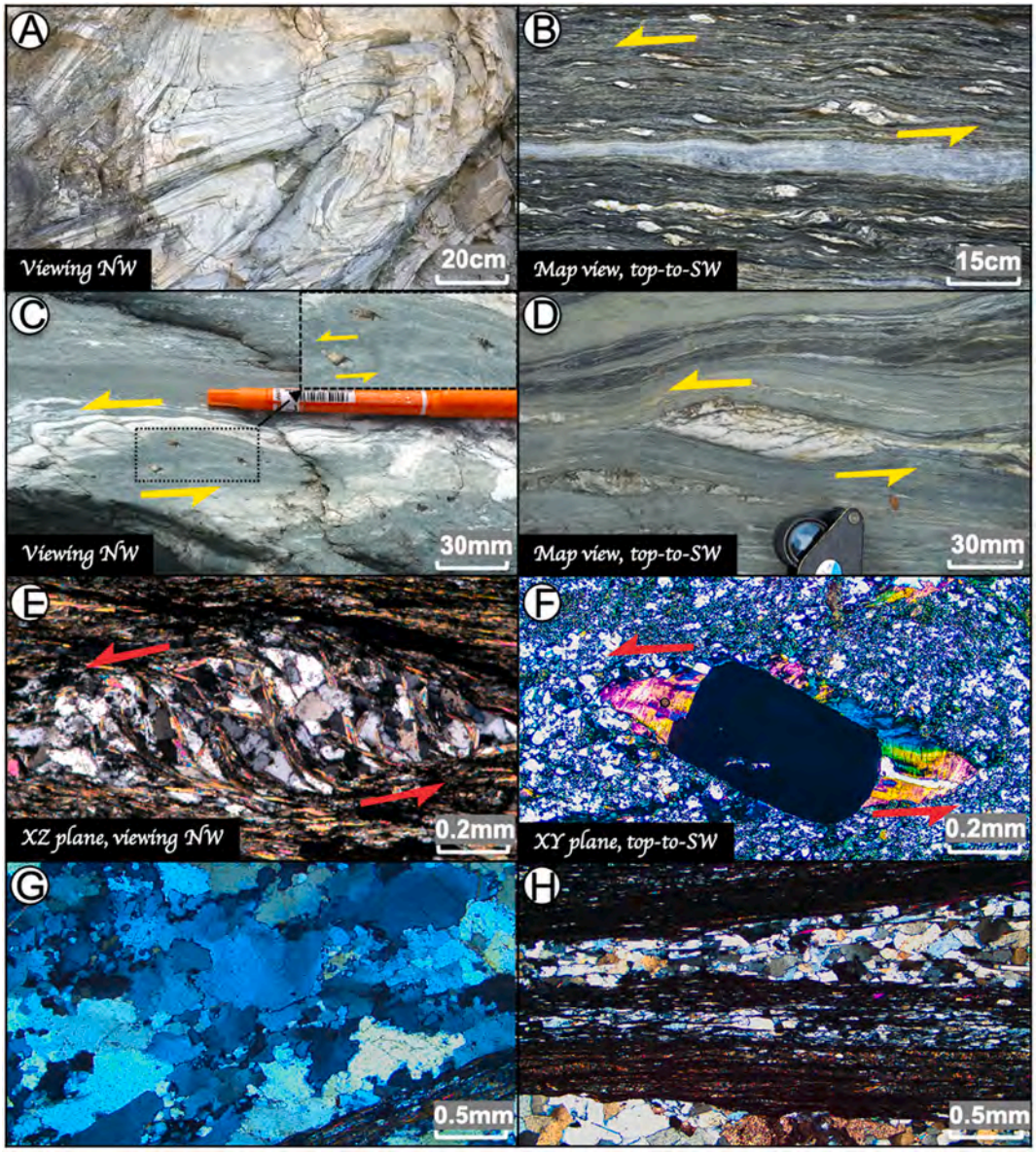

Fig. 2. Field photos and photomicrographs of structures in the high-strain shear zones. Viewing direction is shown in the lower left. A) Mesoscopic tight folds of marble layers indicate strong shearing. B) Mylonitic quartz mica schist with asymmetric lenses of quartz indicating sinistral shear. C) Isoclinal fold in chlorite schist with axial planar cleavage. Inset shows asymmetric strain shadows around pyrite. Asymmetric pyrite shadows with folds indicate top-to-SW, sinistral shear sense. D) Sigma structure defines the sense of shear as sinistral by its stair-stepping wings and inclined fractures. E) S-C foliation within dark and discontinuous C planes and curved Z planes, indicating a top-to-SW, or sinistral, sense of shear. F) Asymmetric pressure shadow showing a sinistral sense of shear. G) Bulging recrystallization is characterized by bulges and small recrystallized grains, showing low-temperature migration recrystallization microstructures. H) The sub-grain boundary rotation recognized by polygonized texture, grain/subgrain sizes and relatively straight grain boundaries along with shear bands suggesting higher relatively temperatures.

psammitic and green, gray, and black pelitic schists (Fig. 2b and c), relatively thick units of marble (Fig. 2a), rare serpentinite/amphibolite (lenticular blocks), and several large bodies of orthogneiss. Although primary sedimentary structures cannot be recognized in the highly metamorphosed Tailuko belt (Fuh, 1962, 1963; Yui and Jeng, 1990; Lu and Hsu, 1992; Tsutsumi et al., 2011), limited number of fossils from the marble and pelitic schist units suggest a late Paleozoic age and Jurassic age of deposition, respectively (Yen et al., 1951; Yen, 1953; Chen, 1989). The different kinds of metamorphosed sedimentary rocks are inferred to have been sourced from Eurasian basement and to represent cover sediments of a Paleozoic to possibly Early Mesozoic passive margin (Yen, 1960; Ho, 1986; Huang et al., 1997; Chen et al., 2016). The large bodies of orthogneisses crop out mainly in the northern part of the Tailuko belt and local exposures of the contact with the country rocks show a clear metamorphic aureole and chilled margins evidencing an intrusive origin. U/Pb zircon ages of the orthogneisses indicate a ~ 200 Ma (early Jurassic) age for an isolated body in the south (Yui et al., 2009) and ~ 88–90 Ma (middle to late Cretaceous) and ~ 200 Ma (early Jurassic) ages for 6–8 large bodies in the north (Lan et al., 2008, 2009; Yui et al., 2009, 2012). The orthogneiss and green pelitic schists are interpreted to be part of a Cretaceous accretionary/subduction system (Wang Lee et al., 1982; Yui et al., 2009, 2012; Chen et al., 2016), which is unconformably overlain by Cenozoic passive margin sediments (i.e., the sedimentary rocks that crop out east and west of the metamorphic core).

The Tailuko Belt generally registers middle to upper greenschist facies as the peak metamorphism (e.g., ~325–425°C/~3–4 kbar) (Ernst, 1983a, 1983b; Ernst and Harnish, 1983; Warneke and Ernst, 1984; Yui et al., 1996; Yui, 2005). However, higher temperatures and pressures have been documented in the orthogneisses and associate aureoles (e.g., up to ~650°C/~8 kbar) (Hwang et al., 2001) and in a few samples from pelitic schists, based on Raman spectroscopy of carbonaceous material (RSCM) (e.g., ~500°C; Beyssac et al., 2007). Combining these available PT data with illite crystallinity (Chen and Wang, 1994; Tsao et al., 1992), and RSCM data sets, it shows generally increasing temperatures from the Slate Belt in the west to the core of the Tailuko Belt in the east, suggesting an inverted metamorphic gradient, and consistent with a mapped overturned syncline, possibly coupled with a few thrust sheets, in the Slate Belt. These data also suggest generally uniform middle to upper greenschist metamorphic conditions in the Tailuko Belt with the few exceptions mapped by Beyssac et al. (2007). Along the southern transect, where the Slate Belt wraps around the southern extent of the Tailuko Belt, the peak metamorphic temperature decreases toward the east, characterized by the maximum temperature dropping steeply from ~475°C in the Tailuko Belt to ~350°C in the Slate Belt.

Early studies of the deformation history of the Tailuko Belt focused on the beautifully exposed outcrop-scale folds and fabrics along two main mountain roads: Highway 8, referred to as the central cross-island highway (CXIH), and Highway 20, referred to as the southern cross-island highway (SXIH). Many of these studies suggested multiple fold and multiple fabric-forming events and often emphasized fold geometries and related fold asymmetry to kinematics without the benefit of additional kinematic indicators (e.g., Stanley et al., 1981; Lu and Wang Lee, 1986). One exception is the work by Lu and Wang Lee (1986), who mapped a series of decametric to metric scale sheath folds in the schists and marbles of the Tailuko Belt. Their structural analysis showed that the folds formed during the second stage of deformation and were associated with a penetrative cleavage, S2, partially by the alignment of grains of biotite and muscovite. This fabric dips steeply southeast and northwest and represents the dominant fabric at most outcrops. Lu and Wang Lee (1986) also argued for progressive horizontal shear parallel to the well-developed lineation, L2, rather than superposed deformation. The work of Lu and Wang Lee (1986), however, did not include a sense of shear for the progressive horizontal shear.

However, more recent structural studies have included detailed kinematic analysis of the ductile deformation of slates, schists, marble and gneisses along both highways. These studies show a progressive change from west-northwest thrusting in the eastern Slate Belt (e.g., Fisher et al., 2002; Faure et al., 1991) to oblique, left-lateral thrusting near the transition to the Tailuko Belt (Clark et al., 1992; Pulver et al., 2002) to dominantly left-lateral strike-slip shearing in the Tailuko (Pulver et al., 2002; Faure et al., 1991). However, Faure et al. (1991) argued that the rocks containing the left-lateral kinematics had been folded and overturned during D2 and D3 and that the original lineation had a northwest trend. The deformation fabrics associated with overturning were not described in detail, and the rotations required for this interpretation appear to be significantly larger than the change in dip across the belt. D3 was also interpreted to be related to back-thrusting (i.e., thrusting to the southeast), following Stanley et al. (1981), although independent evidence for late-stage back-thrusting was not provided. Pulver et al. (2002), working along the CXIH, revealed the transition from down-dip to along-strike stretching as part of D1. Although their L1 and L2 fabrics are parallel and, as we will show below, the kinematics of D2 throughout the Tailuko Belt are also of a significant left-lateral component. As a result, we conclude that both D1 and D2 in the Tailuko Belt exhibited significant components of left-lateral deformation. In the context of these more recent studies, we interpret the sheath folds documented by Lu and Wang Lee (1986) as resulting from left-lateral strike-slip shear during D2.

Exposures along the SXIH also appear to preserve the transition from thrusting to strike-slip deformation. Near the contact between the Slate and western Tailuko Belts along SXIH, Clark et al. (1992) show S2 cross-cutting S1 at a low angle and describe an L2 stretching lineation that plunges moderately northeast. Limited asymmetric pressure fringes around pyrite framboids suggest left-lateral shear (Clark et al., 1992). In the Tailuko Belt east of the transition zone, L2 is sub-horizontal to northeast plunging and associated with left-lateral, strike-slip deformation (Faure et al., 1991; Clark, 1994). As we argue below, we interpret this transition to reflect regional-scale strain partitioning during oblique convergence.

Lu and Wang Lee (1986) also recognized a third penetrative fabric, albeit locally, S3, in the rocks exposed in Tailuko Gorge along the CXIH. Although this fabric set was not studied in detail, Lu and Wang Lee (1986) suggested that it was equivalent to S3 recognized by Stanley et al. (1981) along the SXIH. In this area, S3 dips gently northeast and Stanley et al. (1981) suggested that it formed during southeast-directed thrusting (i.e., back-thrusting in the retro-wedge), although kinematic evidence of thrusting during S3 was not presented. Pulver et al. (2002) also documented a gently northeast-dipping fabric along eastern sections of the CXIH (their Domain I) that is similar to S3 along the SXIH. Pulver et al. (2002), however, considered the fabric to be part of their earliest deformation and labelled it S1. We visited outcrops in the area of Pulver's low-dipping S1 and observed a gently northeast-dipping foliation cutting steeply dipping S2. Although these results are preliminary, and not directly relevant here, we consider the low-dipping foliation and associated lineation in Pulver et al. (2002) Domain I to be S3 and L3, respectively.

North of the CXIH, along the coastline near the village of Suao, Yeh et al. (2016) and Yeh (1998, unpublished MS thesis) mapped two penetrative foliations and associated stretching lineations similar to the S2 and S3 fabrics recognized along the CXIH and SXIH. In the Suao area, however, the fabrics have been rotated approximately 60° CW about a sub-vertical axis, probably by opening of the Okinawa Trough during the last 1 Ma (Angelier et al., 1986; Rau et al., 2008). After removing this rotation, the older foliation recognized by Yeh (1998) strikes northeast and the associated stretching lineation plunges gently SW. Yeh et al. (2016) interpreted the associate kinematics as indicating LL shear, consistent with S2 kinematics in the Tailuko Gorge area. The younger foliation recognized by Yeh et al. (2016) strikes *E*-W and when unrotated dips gently northeast similar to S3.

Between the CXIH and Suao, along the lower reaches of the Hoping River, Jiao (1991, unpublished MS thesis) mapped two structural

domains in the Tailuko Belt. Both domains are characterized by a moderately north to northwest dipping foliation, that is locally mylonitic, and a sub-horizontal stretching lineation. The domains are differentiated, however, by the dip directions of the foliation; an eastern domain is characterized by a foliation that generally dips north whereas a western domain is characterized a foliation that generally dips northwest. Jiao proposed that the different domains represented different deformational events with the western domain preserving D1 structures and the eastern domain preserving D2 structures. Primarily following Stanley et al. (1981)Jiao, 1991 interpreted these two events as representing accretion and back-thrusting, respectively. Alternatively, considering that the Hoping watershed marks the core of the orogenic orocline in the northern Backbone Range (Fig. 1), the two domains may preserve a single deformation with the western and eastern domains representing the western and eastern limbs of the orocline. This interpretation is supported by the fact that when the eastern domain is rotated CCW to remove the oroclinal bending, there is good alignment of both the foliations and lineations across the two domains.

Determining the sense of shear associated with S2 in the Hoping area has been challenging and inconsistencies and different interpretations exist (Jiao, 1991). In both domains recognized by Jiao (1991), however, the stretching lineation consistently has a gentle plunge and the angle between the lineation and the strike of the foliation (i.e., the rake) is small ($\sim < 30°$). The small rake angles argue for strike-slip faulting in both domains unless there have been significant block rotations about non-vertical axes. Although we have argued for rotations about a sub-vertical axis, this type of rotation would not change the magnitude of either the dip of the foliations or plunge of the lineations. We, therefore, propose that the S2 and L2 fabrics are the result of strike-slip faulting and that the eastern domain was rotated CW relative to the western domain during oroclinal bending. We also examined outcrops of the gneissic units along the Hoping River and the Guguzi Coastline and identified various sense of shear indicators (e.g., asymmetric pyrite pressure shadows, elongated clasts, and S-C fabrics) with the majority indicating a left-lateral sense of shear.

Finally, the dominant fabric in the eastern two-thirds of the Tailuko Belt along the orogen (recognized here and in previous studies as S2) generally dips west to northwest whereas the dominant cleavage in the western one-third of the Tailuko Belt (S2) and the Slate Belt, recognized as S1 and locally as S2, generally dips east to southeast. This change in dip across the orogen is often described as part of north-northeast striking cleavage fan (Clark and Fisher, 1995; Tillman and Byrne, 1995; Fisher et al., 2007), although the fan is formed by two different cleavages. Many authors have interpreted the change in dip as evidence for back-folding or thrusting in which the dominant fabric is either tilted (e.g., Faure et al., 1991), flipped (Zhang et al., 2020), or folded (Stanley et al., 1981; Lu and Wang Lee, 1986; Faure et al., 1991) during east-directed flow (Page and Suppe, 1981; Clark et al., 1992; Clark and Fisher, 1995; Fisher et al., 2007). Stanley et al. (1981) also proposed that S3 along the SXIH formed during this stage of back folding. Fisher et al. (2007) interpreted the cleavage fan as reflecting the advection of rocks through a change in regional stress states, induced by the regional-scale geometry of a two-sided wedge. As far as we are aware, however kinematic indicators specifically associated with either back-folding or thrusting have not been presented. Some authors have suggested, alternatively, that the dominant cleavage in the Tailuko was tilted east as the core of the Backbone Range was exhumed, perhaps very recently (Crespi et al., 1996). This interpretation is supported by leveling data across the range which shows a dome shape with decreasing rates of uplift on both flanks of the range (Ching et al., 2011). A third alternative is that eastward tilting of S2 may have occurred during vertical shortening related to exhumation as suggested by the late-stage development and low dip of S3. Thus, the origin of the west dip of the dominant fabric in the eastern two-thirds of the Tailuko Belt is debated. Our main concern here, however, is that the dominant fabric in the Tailuko Belt, S2, initially formed with a relatively steep, and probably vertical, dip.

Estimates of the age of metamorphism and particularly the age of deformation structures has been difficult to constrain in part because appropriate mineral compositions for dating are rare. Also, many of the rocks appear to record multiple sets of deformation fabrics and metamorphic events (Wang and Yang, 1979) making it difficult to differentiate pre- and post-collision/exhumation heating/cooling processes in a quantitative way. Lo and Onstott (1995) carefully characterized the phyllosilicates used for dating in the orthogneisses and showed that a significant fraction was systematically recrystallized and/or replaced by chlorite. They also interpreted second generation rims of phengite and actinolite on hornblendes as Cenozoic age and applied $^{40}Ar/^{39}Ar$ ages of ~6.4 Ma and ~ 7.8 Ma, respectively, for their growth. Also, Wang et al. (1998) proposed that mylonitization of the orthogneiss (interpreted by Jiao (1991) to be S2) occurred 3–4.1 Ma based on the $^{40}Ar/^{39}Ar$ ages of relatively small biotite grains that grew during deformation below their closure temperatures for argon (323–373°C, Wang et al., 1998). The deformation temperatures during mylonitization were interpreted to be ~300° based on the dominance of brittle deformation in feldspar grains while quartz was typically equigranular, suggesting complete recrystallization. These young ages are consistent with $^{40}K/^{40}Ar$ ages of clay fractions of white mica separated from sediments in the Tailuko Belt that range from ~8 Ma to <1 Ma (Tsao, 1996), with completely reset fission track and (U-Th)/He ages of zircon in the orthogneiss (Beyssac et al., 2007) and with reset fission track and (U-Th)/He ages of detrital apatites and zircons (Willett et al., 2003). They are also consistent with $^{40}Ar/^{39}Ar$ ages of 1.6 Ma (Chen et al., 2017b) of pseudotachylite filled veins and faults that cross-cut the fabrics dated by Wang et al. (1998) in the Hoping area.

2.3. Yuli Belt

The Yuli belt consists primarily of two tectonostratigraphic units: 1) a lower grade quartz-mica schist and 2) a generally higher grade "spotted" albite-quartz-mica pelitic schist that typically contains of a variety of metamorphosed blocks of mafic and ultramafic rocks (Yen, 1963). The blocks and their surrounding pelitic schist have experienced blueschist facies (i.e., "high pressure") metamorphism at least locally. The belt overall, however, is characterized by amphibolite to upper greenschist facies metamorphism with peak temperatures and pressures of about 400–550°C and 7–17 kbar, respectively (Liou et al., 1975; Liou, 1981; Chiang, 2003; Beyssac et al., 2008; Baziotis et al., 2017; Tsai et al., 2013; Keyser et al., 2016). Early geochronologic studies of the belt focused on $^{40}K/^{40}Ar$, $^{40}Ar/^{39}Ar$, and $^{87}Rb/^{86}Sr$ geochronologic dating of the metamorphosed mafic rocks and suggested that the belt was mainly metamorphosed during the late Cenozoic (Jahn and Liou, 1977; Jahn et al., 1981; Lo and Yui, 1996; Yui and Lo, 1989), although it was often suspected to have originated from a Mesozoic mélange, the same age as the Tailuko Belt.

More recent dating, however, has shown rather convincingly that the unit was deposited in the Middle Miocene or later, and that high-pressure metamorphism occurred in the latest Miocene, followed by relatively rapid exhumation in Plio-Pleistocene. For example, U/Pb dating of magmatic zircons from the mafic igneous rocks at different localities show consistent middle Miocene ages (15.4 ±0.4 Ma to 16.0 ±0.2 Ma, Chen et al., 2017a; Tsai et al., 2013) and U/Pb dates of detrital zircons separated from the matrix show distributions consistent with deposition ages ranging from the Cretaceous to Mio-Pliocene (Chen et al., 2016; Chen et al., 2017a). In addition, high-resolution Lu-Hf garnet-whole-rock age of a garnet-amphibole schist records crystal growth at 5.1 ±1.7 Ma (Sandmann et al., 2015) and U/Pb dates of zircon rims that are interpreted to record nephrite-forming metasomatism around a serpentinite body at Fengtien suggest growth at 3.3 ±0.7 Ma (Yui et al., 2014). Taken together, these new dates support the interpretation that the belt is a tectonic melange that formed along the Southeast Asia margin, probably contemporaneously with the opening of the South China Sea in the latest Cenozoic, just prior to, and possibly

during the collision.

In contrast, much less research has focused on the structural history of the Yuli Belt as the unit is generally poorly exposed and the limited exposures suggested multiple, complex deformational events. Following one of the most detailed previous studies (Lin et al., 1984) along the Qingshui River in the central part of the Yuli Belt, we can recognize three penetrative fabrics: 1) S1, which is typically parallel to and often obscures lithologic layering, or depositional bedding (S0); 2) S2, which often dips steep to moderate angles and parallels the axial surfaces of tight to isoclinal folds of S1/S0; and 3) S3, which typically dips north at a shallow angle and forms parallel to the axial surfaces of inclined or recumbent folds of S2. Lin et al. (1984) also proposed that S1 generally formed during prograde metamorphism whereas S2, and possibly S3, formed during cooling. Although *syn*-kinematic strain fringes, rotated porphyroblasts and spiral inclusion trails were recognized (Wang and Yang, 1979; Lin et al., 1984, Lin, 1986; Keyser et al., 2016), no systematic study of kinematics associated with the various foliations was presented. A relatively late-forming, shallow-dipping fabric was also documented in mapping of the Yuli Belt in the Guangfu area (Yi et al., 2012) and may be equivalent to the S3 fabric in the Chingshui River area. Interestingly, mapping of structural fabrics along several river sections in the adjacent Tailuko Belt (e.g., the Guangfu area, Yi et al., 2012; the SXIH, Stanley et al., 1981; along the sea cliffs south of Suao, Yeh et al., 2016) and in the eastern sections of the slate (e.g., SXIH, Clark et al., 1992), and suggest that S3 is more regionally extensive than previously appreciated. The possible correlation of the earlier fabrics (i.e., pre-S3) in the Yuli Belt with S1 and S2 fabrics in the Tailuko and Slate Belts remains unknown and certainly deserves to be investigated.

2.4. The contact between the Tailuko and Yuli Belts – The "Shoufeng Fault"

Documenting the character, geometry, and kinematics of the boundary between the Tailuko and Yuli Belts has been hampered by limited exposures of the Yuli Belt and by the general overlap in composition and metamorphic grade of the two units. Although our primary focus is to understand better the deformation history of the Tailuko Belt along the Shoufeng and Wanliqiao Rivers with a particular emphasis on the zones of apparent high strain, the complementary regional-scale, and along-strike observations, can provide additional insights on the contact between the two belts. For example, the contact has traditionally been considered to be a relatively wide structural shear zone (Yen, 1963; Yi et al., 2012; Yui et al., 2012; Chen et al., 2017a), although only recently has a relatively wide zone of deformation been recognized (Yi et al., 2012). Yi et al. (2012) mapped the boundary as a zone of deformation, up to 2 km wide, the "Daguan Schist" extending from the Wanliqiao River to the approximate latitude of Ruisui village in the Longitudinal Valley (Fig. 1). The zone appears to record a high degree of strain and includes zones of mylonitization. Although kinematic data were not provided in Yi et al. (2012), we tend to interpret the zone recorded significant left-lateral strike-slip ductile shearing, based on our own field observations and those from Ho (2007, unpublished MS thesis).

For the high strain zones along the Shoufeng and Wanliqiao Rivers and along rivers and highways that we examined during several attempts of reconnaissance fieldwork, the high strain zones generally occur in gray or black schists that crop out east of the easternmost thick marble unit. Because occurrence of extensive outcrops of marble being attributed to the Tailuko Belt, one interpretation is that the shear zones mark the contact between the two units, as Yi et al. (2012) suggested. This generalization appears to break down along the CXIH, however, because left-lateral deformation and associated high strain, marked in part by the occurrence of sheath folds, occurs both east and west of the main marble unit. Clark et al. (1992) also suggested that left-lateral ductile deformation observed along the SXIH transitions from down-dip stretching in the Slate Belt to along-strike stretching in the Tailuko Belt west of the main marble units. We propose, therefore, that left-lateral shear is a characteristic feature of the Tailuko Belt and that the contact with the Yuli Belt also is a left-lateral zone of deformation. More detailed mapping of the Yuli Belt, which is characterized in part by the occurrence of Late Miocene and younger detrital zircons (Chen et al., 2017a), will test this hypothesis and provide critical insights into the history of both belts.

3. Structural fabrics and paleotemperature data from the Tailuko Belt

3.1. Structures along the Shoufeng and Wanliqiao Rivers

The Shoufeng and Wanliqiao Rivers in the central part of the eastern slope of the Backbone Range provide good and rather continuous exposures through over eastern half of the Tailuko Belt, yielding opportunities for correlating lithologic units and structural patterns in 2-D and even 3-D views (Fig. 3). We, in particular the first author, completed several mapping and sampling expeditions along both rivers over a collective period of about 15 weeks, from 2007 to 2015, and 2018 to 2019 (Fig. 3) (e.g., Ho, 2015; Lee et al., 2019). Meso- and microscopic observations show that the most penetrative fabric S2, which can be regionally traced throughout the field areas, cuts S0/S1 (often crenulated or folded at different degrees) and developed shear structures. S0/S1 are only preserved residually in the microlithon domain of S2 and/or in the hinge zone of D2 folds. Based mainly on these expeditions, Ho and Lo (2015) mapped a re-folded, regional-scale fold near the headwaters of the Shoufeng River; and documented the progressive development of three penetrative fabrics, S1, S2 and S3. They also proposed that the fold represented a type-1 and type-3 interference pattern (Fig. 3). We complemented these studies with several field expeditions in 2018 and 2019 and focus here on characterizing: 1) the penetrative fabric that dominates many of the outcrops along both rivers, S2, and 2) the high strain zones that appear to be associated with S2 (Fig. 2a and b).

The outcrops along both rivers consist of inter-layered marble, greenschist, and black schist, typical of the Tailuko Belt and expose both meso-scale folds and zones of relatively high penetrative shear strain (Fig. 2c and d). The dominant lithologic layering, which represents the superposition of S2 on S1 and/or S2 on S0, dips steeply to moderately west-northwest; that is, the teconostratigraphy generally forms a northwest-dipping homocline. Local reversals in the apparent stratigraphy also suggest outcrop- to regional-scale isoclinal folds, although these are relatively rare. Parts of the mapped sections interpreted as zones of relatively high shear strain are characterized by a much greater disruption of the local stratigraphy and a more penetrative foliation relative to outcrops outside of shear zones. The zones also often display lenses or stringers of quartz vein and marble in a highly foliated green- or gray schist, suggesting relatively high strain. Multiple zones of apparent high strain are exposed along both the Shoufeng and Wanliqiao Rivers (Fig. 3) and one or two of the zones may correlate between the watersheds (Fig. 3). Detailed structural analyses, presented below, suggest that the high strain zones are part of D2 deformation event.

Many of the outcrops along both rivers also display a low-dipping foliation that crosscuts S2 (even at localities where S2 becomes a shallow-dipping plane) and is identified as S3 (Ho and Lo, 2015). Although not studied in detail, S3 appears to form a broad, antiformal structure that plunges gently north to northeast. Normal faults, extensional quartz-filled veins, and recumbent folding of S2 with S3 forming an axial planar cleavage suggest a possible transition to sub-vertical shortening and NE extension at the shallow crust levels.

Foliation, lineation and kinematic data associated with S2 were collected along both rivers where ever possible, yielding approximately 600 structural measurements. Approximately 400 oriented slabs of rock samples ranging from 1 kg to 5 kg were also collected for more detailed laboratory analyses. The stretching lineation L2 on the dominant foliation S2, was identified in the field by a variety of features, including

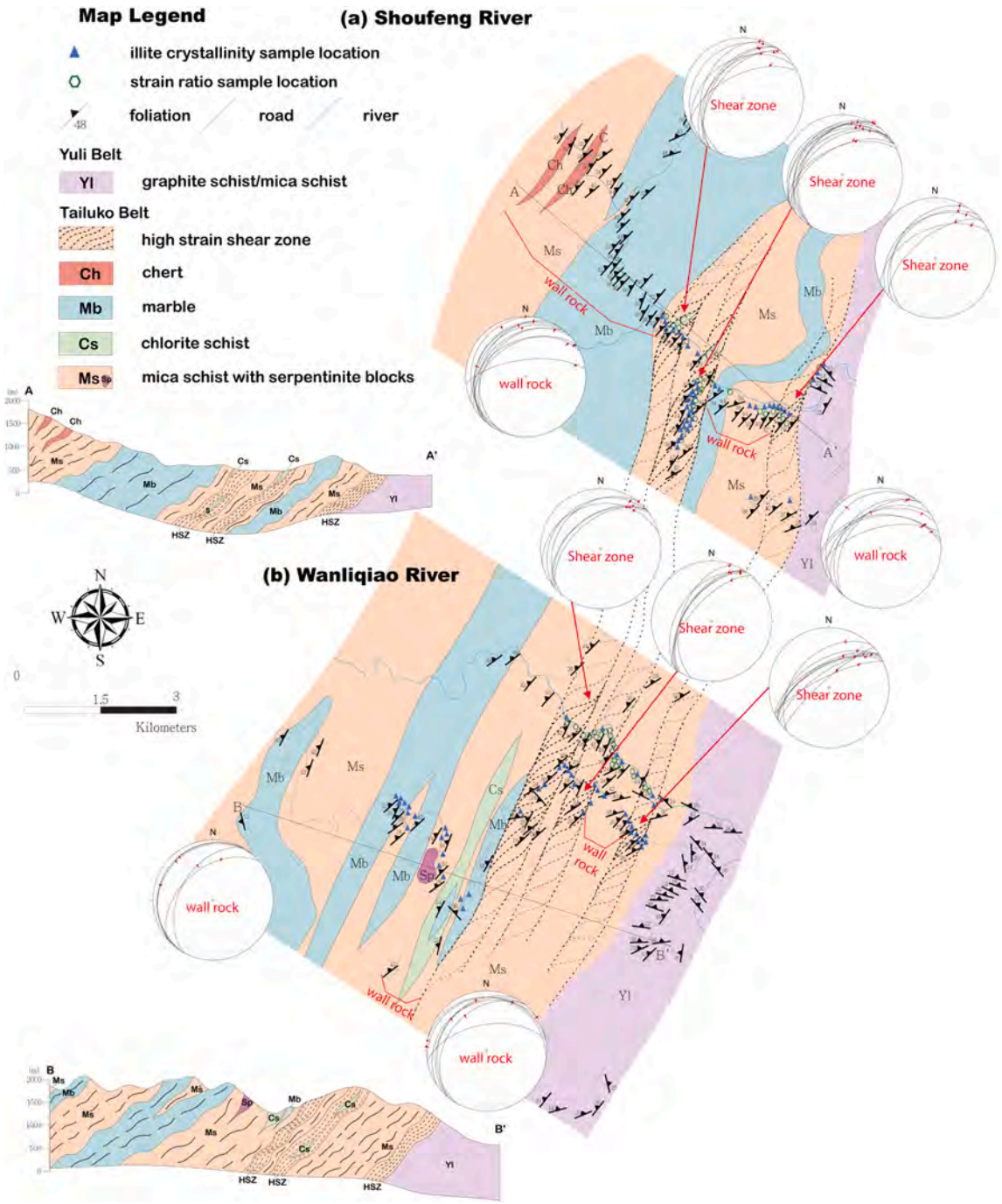

Fig. 3. Detailed geologic maps and profiles with structural data and sample locations in the (a) Shoufeng and (b) Wanliqiao River areas. Stereonets show dominant fabric and associated lineation (interpreted as S2 and L2, respectively) in zones of apparent high shear zones and wall rocks. Note tighter clustering of lineations in high strain zones and slight deflection of fabric strikes (highlighted by lens-shaped patterns within the zones of high strain. See index map in Fig. 1 for the location of the sites. Unit Yl represents Yuli Belt; all other units are Tailuko Belt.

flattened and elongated quartz clasts (Fig. 2d), S-C fabrics (Fig. 2e), pressure fringes (Fig. 2f), and clusters of elongate phyllosilicates. The stretching lineation, L2, is inferred to represent X of the long axis of the strain ellipsoid associated with development of S2 fabrics, where X > Y > Z; note that S2 is inferred to represent the X-Y plane. In cases where it was not possible to recognize or identify L2 in the field, oriented samples were cut parallel to S2, which typically exposed L2. Field and laboratory measurements of S2 and L2 were then tabulated and plotted on stereonets. All oriented samples were also cut parallel to the stretching lineation and perpendicular to S2; that is, parallel to the X-Z plane. These slabbed surfaces and thin-sections were used to characterize S2 and L2, to measure the orientations and aspect ratios of quartz and feldspar grains, and to document the kinematics (sense of shear) associated with S2.

3.2. *Structural fabric data*

Along both Shoufeng and Wanliqiao Rivers, S2 dips generally WNW and L2 and plunges gently NE, although the both data sets show dispersion. The wide dispersion appears to decrease significantly in the areas of inferred high strain. For example, outside the zones considered to represent high strain the trend of L2 ranges from 280° to 80°, whereas

in the high strain zones L2 ranges from 030° to 060° (Fig. 3). The poles to S2 show a similar tightening within the zones of inferred high strain.

The aspect ratios of siliceous phases (primarily quartz and feldspar) inside and outside the zones of apparent high strain also show systematic changes. The ratios were measured using black-and-white photographs of thin-sections and slabs parallel to the X-Z plane (Stipp et al., 2002). Ratios were calculated using the SURFOR method (Panozzo, 1987) where the number of grain boundary intercepts are plotted radially resulting in a sinusoidal curve. A total about 800 pictures were taken from oriented slabs in order to analysis aspect ratios. Image processing were then enhanced by Adobe Photoshop and calculated on grain boundaries with Image-Pro Plus. The difference between the trough and crest represents the fabric aspect ratio and the coordinates are taken as the orientations of the long and short axes of the fabric ellipse. Interestingly, samples collected from the zones of inferred higher strain are significantly higher with an average ratio of 1.95 ±0.30 (see Appendix A) than samples from outside the zone which yield an average ratio of 1.59 ±0.15 (Fig. 4, see Appendix A). These results are consistent with field-based interpretation that the zones represent areas of relatively high strain.

Observations of thin-sections, slabbed surfaces and outcrops parallel to the X-Z plane were all used to document the kinematics, or sense of shear, associated with S2. Kinematic indicators in the zones of relatively high strain are particularly well-developed, including asymmetric folds, strain fringes around pyrite ore magnetite, S-C structures, imbricated layering, R and R' shears, sigmoidal core-and-mantle structures and insolvable residues associated with pressure solution. In cases where the asymmetry could be determined, 80–90% indicated a left-lateral sense of shear. This result is consistent with kinematic analyses outside the high strain zones farther north within the Tailuko Belt in the Hoping River and Tailuko Gorge areas (e.g., Jiao, 1991; Pulver et al., 2002) and with quartz/chlorite shadows around pyrite framboids in the Slate Belt near the Tailuko Belt along the SXIH (Clark and Fisher, 1995). Conand et al. (2020) have also recently documented significant left-lateral deformation in part of the southern Backbone Range. The results presented here are consistent with those from Conand et al. (2020), although we propose that the left-lateral ductile D2 deformation is concentrated in the metamorphic core, especially in the eastern half of the Tailuko Belt, and that it is no longer active. In contrast, Conand et al. propose that the style of deformation changed from concentrated strike-slip to more distributed deformation associated with transtension, a deformation event probably later than D2 event in the metamorphic core.

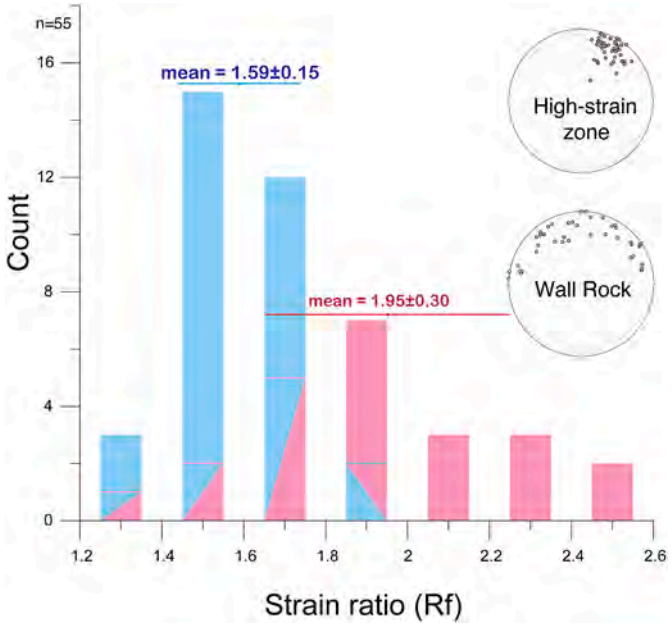

Fig. 4. Aspect ratios (geometric long/short axes) of grains measured in XZ sections (see text) and structural fabric data and from zones of inferred high strain (pink) and wall rocks (blue) along the Shoufeng and Wanrung River areas. Means and standard deviations are also shown. Stereonets show trend and plunge of stretching lineations in and outside of zones of high strain. The zones of inferred higher strain have higher aspect ratios and tighter clustering of lineations, consistent with higher shear strain in these zones. (For interpretation of the references to colour in this figure legend, the reader is referred to the web version of this article.)

3.3. Illite crystallinity and paleotemperature

Approximately 91 samples of fine-grained phyllite were also collected in the areas of the Shoufeng and Wanliqiao Rivers for illite crystallinity (IC) analysis. The locations of the samples are widespread across the Tailuko Belt (Fig. 3), including the zones of apparent high strain. To measure accurate IC values, uniform sample preparation is necessary, and we followed procedures developed by Kisch (1990). The samples were washed and dried, then disaggregated with a jaw crusher and sieved (<100 mesh). About 20 g of the sieved clay minerals were stirred into 250 ml deionized water, and additional disaggregation was achieved with an ultrasonicator for 30 min. To remove the influence from detrital muscovite, 2-μm clay size fractions were separated by gravity, settling for ~3.5 h. The supernatant was dripped on a small glass section and dried in a low temperature (< 50°C) oven. Once dry, the mounts were scanned from 5° to 15° 2θ, with scan rate at 1° 2θ/min by CuKα scintag X-ray powder diffractometer at National Cheng Kung University. A calibration curve was established by scanning the standard specimens from Tsao (1996) and Kisch (1990). IC values were determined automatically, measured as FWHM of the illite (001) peak by Jade software (Jade Software Corp., Jacksonville, FL, USA).

The IC values from the two field areas (i.e., Shoufeng and Wanliqiao Rivers) range from 0.15 to 0.34 Δ°2θ, with a mean of 0.23 ±0.04 (n = 91) and are consistent with previous studies of illite crystallinity elsewhere in the Tailuko Belt. However, the spread in IC values is noticeably higher. For example, a regional-scale study by Tsao et al. (1992), following similar sample and processing techniques, yielded relatively uniform values ranging from 0.19 to 0.23 and a mean of 0.21 ±0.01. To better understand the wide range in IC values, we separated the samples into two groups: 1) samples from the field-identified shear zones (SZ, see Appendix B) and 2) samples classified as wall rock (WR, see Appendix B). The resulting histograms show distinct groups with lower IC values characterizing the samples from the shear zones (Fig. 5).

Illite crystallinity values are commonly used as a geothermometer (Kubler, 1968), although weathering, circulating fluids, and deformation can modify IC values, masking or altering initial temperatures. With these caveats, we correlated the IC values with temperature based on the work of Verdel et al. (2011) and Merriman and Frey (1999). This correlation suggests that the Tailuko Belt in the Shoufeng and Wanliqiao areas experienced paleotemperatures up to 400°C. In addition, higher paleotemperatures (50°C higher on average) are more common in zones characterized by relatively high shear strain (Fig. 5). We interpret these slightly higher paleotemperatures to reflect heating by hot fluids during or after the zones formed or by frictional heating related to slip during deformation.

The maximum paleotemperatures from the Shoufeng/Wanliqiao area are generally consistent with previous studies of IC values along the CXIH and SXIH (Tsao, 1996) and with a regional-scale study of IC that Chen and Wang (1995) used to construct the metamorphic facies map of Taiwan (Chen and Wang, 1994). The maximum temperatures inferred from the IC data for all three studies are noticeably lower than the maximum temperatures interpreted from RSCM along these two highways. For example, RSCM data from the central part of the CXIH, near the village of Tienshiang, indicate maximum temperatures close to 500°C. One possibility is that these higher temperatures also reflect

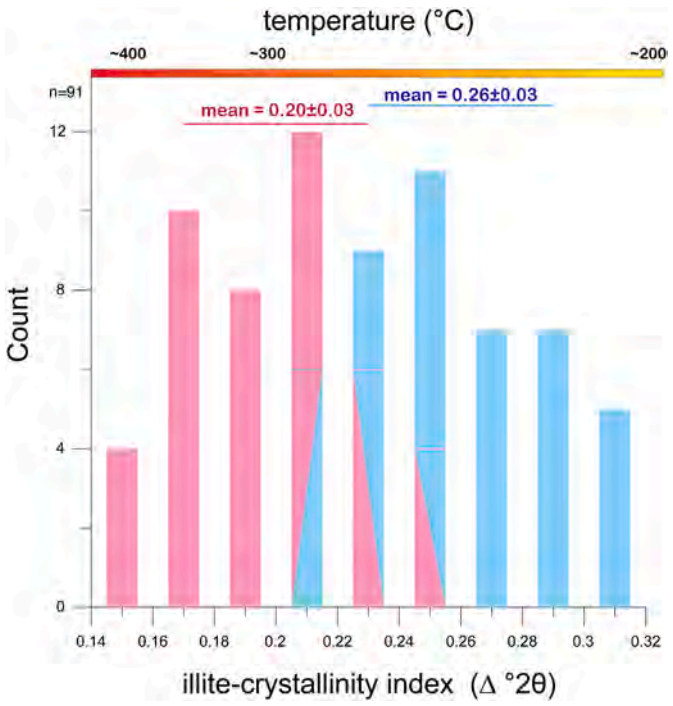

Fig. 5. Histograms and normal distribution of illite crystallinity values with means and standard deviations from the zones of inferred high strain (pink) and wall rocks (blue). Paleotemperature bar is compiled from Merriman and Frey (1999) and Verdel et al. (2011) and suggests higher paleotemperatures in the zones of inferred high strain relative to the wall rocks; for example, ~400°C in zones of high strain versus less than 300°C in wall rocks. (For interpretation of the references to colour in this figure legend, the reader is referred to the web version of this article.)

strain heating or the migration of fluids during or after deformation. Alternatively, because the RSCM-based maximum temperatures are consistently higher, even at lower metamorphic grades, the different techniques may be measuring maximum temperatures at different times, from events in the source areas to burial metamorphism to recrystallization during deformation. At present, we are not able to differentiate these different possibilities.

4. Field studies of the Tailuko Belt at different latitudes

To understand the possible regional significance of the left-lateral deformation and the high-strain zones recognized along the Shoufeng and Wanliqiao Rivers, we examined outcrops in four additional areas at the different latitudes along strike in the eastern Backbone Range: 1) the lower reaches of the Hoping River and along the Guguzi Cliffs; 2) the CXIH; and 3) the SXIH, including the nearby Dalun and Xinwulu Rivers; and 4) the Taimali River. In all four areas S2 and L2 were identified in outcrops and/or oriented samples, and the sense of shear was documented where possible.

4.1. The lower reaches of the Hoping River and along the Guguzi Cliff

We examined outcrops along Hoping River and Guguzi Cliffs, coastal cliffs a few km south of the mouth of the Hoping River, that expose orthogneiss with a variably developed mylonitic fabric. In both areas the fabric dips moderately north and displays a well-developed stretching lineation that plunges gently west-southwest (see also Korren et al., 2017). The fabric and lineation are interpreted to be S2 and L2, respectively (Jiao, 1991, discussed above). The outcrops along the Hoping River also expose well-studied examples of pseudotachylite-filled faults and veins that cross-cut the mylonitic fabric (Korren et al., 2017). In both areas, we collected as many kinematic indicators as possible on the X-Z plane of strain for D2. About 80% of the features yielded a left-lateral sense of shear (Fig. 1).

4.2. Outcrops along the central cross-island highway

Penetrative S2 and L2 are well-developed in the Liwu River along the CXIH where Lu and Wang Lee (1986) identified F2 sheath folds and Pulver et al. (2002) documented the transition from down-dip to strike-parallel shear. We examined multiple rock surfaces parallel to the inferred XZ planes associated with S2 and our kinematic indicators showing a left-lateral sense of shear consistent with Pulver et al. (2002) and Faure et al. (1991). The areas of left-lateral ductile shear extend from 1 to 2 km west of Loshao, through the area around Tienshiang to near the Buluwan Village. That is, rather than distinct zones of concentrated deformation, left-lateral ductile deformation appears to be characteristic feature of the entire Tailuko Belt in this area. Interestingly, left-lateral ductile deformation is recorded on both limbs of the "cleavage fan" just west of Loshao that in this area is defined changes in dip of S2, arguing that tilting or folding of S2 occurred after rocks were deformed by D2/S2 (Pulver et al., 2002; Faure et al., 1991).

We also examined outcrops in domain I (i.e., the eastern part of the Tailuko Belt) of Pulver et al. (2002) and recognized a gently north dipping penetrative foliation S3 that cross-cuts a steeply plunging, isoclinal D2 fold. On the limbs of this fold, the low-dipping foliation S3 is axial planar to generally cylindrical folds with gently plunging axes. In the hinge area, however, the intersection of the gently dipping cleavage S3 with the steeply plunging D2 folds produces a dome-and-basin interference pattern. This is the main reason why we interpret the low-dipping foliation as S3, and, although not relevant here, propose that Pulver et al. (2002) misidentified S1 in this area.

4.3. Outcrops along the south cross-island highway

Stanley et al. (1981) first reported the history of metamorphic fabrics and the development of ductile shear zones along the SXIH and Xinwulu River, although kinematic indicators were not recognized at that time. In our complementary fieldwork, we were able to revisit outcrops of Stanley's "imbricate thrust zone" that separates the Yuli and Tailuko Belts (stop 4, Fig. 1 and map in Fig. 3, Stanley et al., 1981). The zone displays a northwest, moderately dipping S2 in green and black schists as well as structural features suggestive of high strain (e.g., stringers and lenses of quartz, R and R' shears, outcrop-scale imbricate horses, and a relatively well-developed foliation). We also identified a sub-horizontal stretching lineation, L2, associated with S2. The outcrop surfaces parallel to L2 and perpendicular to S2 display numerous asymmetric structures, for example, the strain fringes, S-C fabrics, and R and R' shears. About four fifths of our observations from the zone indicate a left-lateral sense of shear. We also expanded our reconnaissance field observations along-strike by incorporating observations from the Dalun River, which drains north and feeds into the Xinwulu River (see also Fig. 3, Stanley et al., 1981). These exposures provided additional sense of shear indicators (e.g., asymmetric pyrite pressure shadows and sigmoidal en échelon quartz veins) showing consistent left-lateral shear.

4.4. Structures along the Tamali River

This southernmost transect along the Tamali River comprises Eocene to Miocene cover rocks of the Pilushan, Lushan and Chaochou Formations that have been correlated with units in the Slate Belt to the northwest. The lithologies and sedimentary features suggest different depositional environments for at least some of the sequences. For example, some of the units suggest deposition by turbidity currents and may have been deposited in relatively deep water compared to the continental shelf deposits in the Slate Belt. In any case, mapping along the Taimali River shows three tectonostratigraphic units separated by

relatively large (meters to tens of meters) zones of high deformation. The tectonostratigraphic units are characterized by different fabric geometries and intensities. The western and central units display a slaty-like cleavage that dips moderately although the dip directions are different; in the western unit, the cleavage dips east-southeast whereas in the central unit the cleavage dips southwest. The cleavage in the eastern unit is more schistose and dips gently, forming a gentle, north-trending dome.

The two deformation zones separating the three tectonostratigraphic units are intensely deformed by brittle structures with both strike-slip and normal faults. A paleostress analysis shows that both zones record an early phase of left-lateral strike-slip faulting along generally steep, north-striking surfaces, overprinted by normal faulting along new or reactivated slip surfaces that are also generally north striking.

Importantly, these newly recognized zones of deformation project northward to the eastern and western boundaries of the Tailuko Belt (Mesalles, 2014). We, therefore, propose that the zones of brittle, strike-slip deformation correlate with the ductile strike-slip shear in the Tailuko belt but represent deformation at higher structural levels where ambient temperatures are expected to be lower. The occurrence of more schistose rocks east of the eastern shear zone suggests a correlation with the Yuli Belt and is consistent with the hypothesis that strike-slip deformation occurred in both the metamorphic basement and the overlying sedimentary cover.

5. Discussion and conclusions

New field and structural data presented here, integrated with complementary data along strike at the different latitudes in the metamorphic core, particularly the Paleo-Mesozoic Tailuko Belt, suggest a consistent pattern of left-lateral strike-slip deformation along the entire length of the orogen. This regional-scale deformation was accommodated by 1) ductile deformation and mylonitization at mid-crustal levels and 2) brittle deformation and CCW block rotations at upper-crustal levels. This regional deformation appears to have occurred in the latest Pliocene (~ 4.1 to 3 Ma) based on $^{40}Ar/^{39}Ar$ ages of mylonitic shear zones (Wang et al., 1998).

A generally similar deformation history was previously recognized by several researchers, such as Clark (1994), Clark et al. (1992), Pulver et al. (2002), and Mondro et al. (2017), although Pulver et al. (2002) and Mondro et al. (2017) argued for a component of lateral extrusion and Clark (1994) and Clark et al. (1992) presented limited kinematic data from the Tailuko Belt. Conand et al. (2020), Mouthereau et al. (2019) and Malavieille et al. (2019) presented evidence of orogen-scale strain

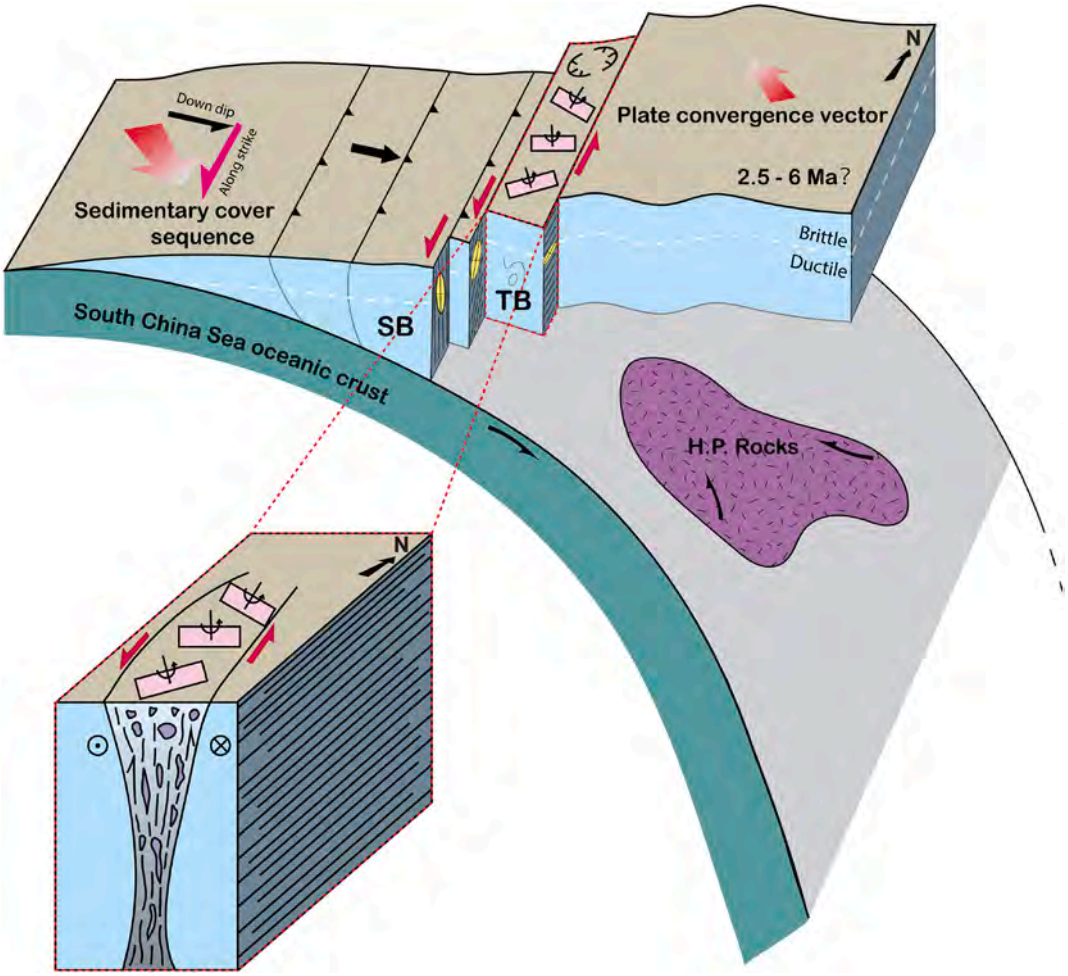

Fig. 6. 3-D tectonic model showing strain partitioning during highly oblique plate convergence (large red arrow). Oblique convergence is partitioned into a generally down-dip component, evidenced by down-dip stretching in the Slate Belt (yellow ellipse on SB) and an along-strike component, evidenced by along-strike stretching in the Tailuko Belt (yellow ellipse on TB). The moderately plunging yellow ellipse between SB and TB presents the transition in lineation plunge between the two belts (see text). Sheath folds are also depicted schematically on TB. The inset shows the relation between ductile shear in the Tailuko Belt and block rotations observed in southern Taiwan. Left-lateral shear is interpreted to be recorded by ductile fabrics in the Tailuko Belt and by block rotations at shallower structural levels. This deformation is also interpreted be contemporaneous with development of the Slate Belt. See index map in Fig. 1 for the general view direction of the 3-D model. (For interpretation of the references to colour in this figure legend, the reader is referred to the web version of this article.)

partitioning in the Taiwan orogen; however, their interpretations integrated past and present kinematic data. Here, we argue for a distinct phase of strain partitioning that ended younger than 3 Ma, whereas strike-slip deformation was limited to the Tailuko Belt and structurally shallower sedimentary units to the south (e.g., the sedimentary cover rocks and Slate Belt, of southern Taiwan).

At an island-wide scale, left-lateral strike-slip deformation occurred in the metamorphic core of the orogen is nearly contemporaneous with deformation in the Slate Belt west of the metamorphic core, although the kinematics are substantially different. For example, the Slate Belt incorporates sediments of Middle to Late Miocene age and *syn*-kinematic veins of muscovite and corrensite yield ages range from 6 to 2.5 Ma (Chen et al., 2016). Importantly, this age range includes the $^{40}Ar/^{39}Ar$ ages of the mylonization in the Tailuko Belt (3–4.1 Ma, Wang et al., 1998) and is compatible with the age of the pseudotachylite veins that cut the mylonites (Chen et al., 2017b). The kinematics of the deformation in the western Slate Belt, however, indicate top-to-the west-northwest thrusting and imbrication with limited evidence of strike-slip deformation. To reconcile the overlap in ages of deformation and the differences in kinematics, we propose that during the late Pliocene, highly oblique plate convergence was partitioned into orogen-parallel and orogen-perpendicular components (Fig. 6).

Oblique plate convergence and partitioning in the early Taiwan orogen are consistent with nearly all of the more recent plate reconstructions for the late Cenozoic. A fundamental constraint on all of the reconstructions is the northward motion of the Philippine Sea Plate relative to Eurasia throughout much of the Cenozoic which implies significant left-lateral motion along the Eurasian margin. Essentially all of the reconstructions also show a change in motion of the Philippine Sea Plate from its earlier northward motion to a west-northwest direction in latest Cenozoic. Although the timing of this change in motion is not well constrained, the most recent, and arguably the most thorough evaluation of the motion of the Philippine Sea Plate, argues for a change in motion less than 2 Ma. The data presented here are consistent with this very recent change in motion of the Philippine Sea Plate with respect to Eurasia.

We also need to address any first-order deformational features that post-date the D2 deformation event, characterized primarily by S2 a penetrative foliation that dominates most outcrops of the Tailuko Belt, and reconcile any consequences these later events may have had on S2. In particular, S3 is a regionally extensive and, at least locally, a penetrative fabric that deforms or overprints on S2. Although S3 has not been studied in detail, that the authors are aware of, it consistently dips gently northwest or northeast. The low dip of S3 argues for significant vertical shortening and/or substantial sub-horizontal stretching. The only relatively abundant strain indicators associated with S3 are a suite of quartz-, calcite- and locally adularia-filled veins that developed late in the history of D3/S3 (Chojnacki et al., 2019). The veins consistently strike northwest and dip steeply, indicating northeast-southwest extension. Kinematic indicators are more limited and suggest both top-to-the northeast and top-to-the southwest parallel to S3. Based on these rather limited observations we propose that vertical shortening and possibly to-top-the-northeast shear deformed S2 from its initial vertical orientation to a more moderate dip. We prefer a top-to-the northeast shear because an initially vertical shear zone would rotate clockwise (viewed to the north), resulting in a northwest dip, which is what is observed today. The obliquity of the shear during D3, relative to the more northerly striking S2 shear zone, may have resulted in a series of en echelon segments (Fig. 1) rather than a through-going shear zone one would expect initially. Our regional reconstruction therefore depicts a vertical shear zone that generally strikes 030.

Additional deformation events that may have affected the strike-slip regime that characterizes the main ductile deformation in the Tailuko Belt, include structures associated with the deformation and emplacement of the Yuli Belt. This belt includes 'exotic' mafic blocks that preserve evidence of high-pressure metamorphism (~50 km, Baziotis et al., 2017; Keyser et al., 2016; Tsai et al., 2013) and limited geochronologic data suggest peak metamorphism occurred 6 to 5 Ma (Sandmann et al., 2015). This unit was subsequently juxtaposed against the Tailuko Belt, possibly during the oblique convergence described here, but the process (es) and associated accommodating structures responsible for this juxtaposition have not been identified. The Yuli Belt is also characterized, at least in part, by a low-dipping, penetrate foliation that may be equivalent to S3 recognized in the Tailuko Belt. The role that this fabric played in exhumation of the Yuli Belt, and/or the Tailuko Belt, has not been evaluated. The processes associated with uplift and exhumation of the Tailuko Belt, relative to the nearby western and eastern slate belt, are also unknown.

The boundary between two metamorphic belts has previously been reported as the Shoufeng Fault (Yen, 1963). However, as discussed above, the actual location, motion, and kinematics associated with the Shoufeng Fault are topics of active research (e.g., Yi et al., 2012; Ho, 2015; Lee et al., 2019). More detailed work, including constraining the maximum age of depositional units using detrital zircon U-Pb dating may show that the high strain zones recognized in this study close to the Tailuko-Yuli contact are the "Shoufeng Fault" (Yui et al., 2012; Chen et al., 2017a). Additional finite strain data may also illuminate new shear zones equivalent or complimentary to the Shoufeng Fault.

Finally, the orogenic orocline in northeastern Taiwan, where the mylonitic rocks of the Tailuko Belt bend nearly 70–80° CW relative to the core of the orogen documents relatively young, regional-scale deformation. In fact, many of these late fabrics and structures may be related to the transition from a regime dominated by strain partitioning during oblique plate convergence in the Pliocene to a regime dominated by orogenic shortening and uplift in the Pleistocene.

CRediT authorship contribution statement

Gong-Ruei Ho: Conceptualization, Investigation, Methodology, Data curation, Validation, Formal analysis, Visualization, Writing – original draft, Writing – review & editing. **Timothy B. Byrne:** Conceptualization, Investigation, Methodology, Formal analysis, Funding acquisition, Resources, Supervision, Visualization, Writing – original draft, Writing – review & editing. **Jian-Cheng Lee:** Conceptualization, Investigation, Formal analysis, Funding acquisition, Project administration, Resources, Supervision, Visualization, Writing – review & editing. **Lucas Mesalles:** Data curation, Investigation, Writing – review & editing. **Ching-Weei Lin:** Conceptualization, Funding acquisition, Project administration, Resources, Supervision. **Wei Lo:** Conceptualization, Funding acquisition, Project administration, Resources, Supervision. **Chung-Pai Chang:** Conceptualization, Supervision.

Declaration of Competing Interest

The authors declare that they have no known competing financial interests or personal relationships that could have appeared to influence the work reported in this paper.

Acknowledgment

We greatly appreciate the assistance of Kuo-Wei Chang and his mountain guides during various stages of the fieldwork; the outcrop discussions with Wei-Hao Hsu, Jon Lewis and his students, Lindsey Aman, Lauren Donati, Ross Bolesta, and Susan Adams as well as graduate student, Mike Chojnacki, from the University of Connecticut, and the innovative ideas from the Yuli Exhumation Study Team (YES Team). Byrne greatly appreciates the quiet space at NDHU provided by Dr. Chin-Ho Tsai and Dean Wen-Yen Chang during the final stages of manuscript preparation. This research was supported by grants from the Ministry of Science and Technology (MOST) of Taiwan (MOST 107-2116-M-001-026-MY3; MOST 110-2116-M-001-004 to Jian-Cheng Lee and MOST 109-2811-M-259-513 to Chin-Ho Tsai) and the US National Science

Foundation (EAR-1220453 to Byrne). This is a contribution of Institute of Earth Sciences, Academia Sinica, IESAS-2406.

Appendix A. Supplementary data

Supplementary data to this article can be found online at https://doi.org/10.1016/j.tecto.2022.229332.

References

Angelier, J., Barrier, E., Chu, H.T., 1986. Plate collision and paleostress trajectories in a fold-thrust belt: the foothills of Taiwan. Tectonophysics 125 (1–3), 161–178. https://doi.org/10.1016/0040-1951(86)90012-0.

Baziotis, I., Tsai, C.H., Ernst, W.G., Jahn, B.M., Iizuka, Y., 2017. New P–T constraints on the Tamayen glaucophane-bearing rocks, eastern Taiwan: Perple_X modelling results and geodynamic implications. J. Metamorph. Geol. 35 (1), 35–54. https://doi.org/10.1111/jmg.12218.

Beyssac, O., Simoes, M., Avouac, J.P., Farley, K.A., Chen, Y.G., Chan, Y.C., Goffé, B., 2007. Late Cenozoic metamorphic evolution and exhumation of Taiwan. Tectonics 26 (6), 1–32. https://doi.org/10.1029/2006TC002064.

Beyssac, O., Negro, F., Simoes, M., Chan, Y.C., Chen, Y.G., 2008. High-pressure metamorphism in Taiwan: from oceanic subduction to arc-continent collision? Terra Nova 20 (2), 118–125. https://doi.org/10.1111/j.1365-3121.2008.00796.x.

Chang, C.P., Angelier, J., Lee, T.Q., Huang, C.Y., 2003. From continental margin extension to collision orogen: structural development and tectonic rotation of the Hengchun peninsula, southern Taiwan. Tectonophysics 361 (1), 61–82. https://doi.org/10.1016/S0040-1951(02)00561-9.

Chang, C.P., Angelier, J., Lu, C.Y., 2009. Polyphase deformation in a newly emerged accretionary prism: folding, faulting and rotation in the southern Taiwan mountain range. Tectonophysics 466 (3), 395–408. https://doi.org/10.1016/j.tecto.2007.11.002.

Chen, Z.H., 1989. A Preliminary Study of the Fossil Dinoflagellates from the Tananao Schist, Taiwan (Master). National Taiwan University, Taipei.

Chen, C.T., Wang, C.H., 1994. Metamorphic Facies Map of Taiwan. Special Publication of the Central Geological Survey, 2.

Chen, C.T., Wang, C.H., 1995. Explanatory Notes for the Metamorphic Facies Map of Taiwan. Special Publication of the Central Geological Survey, 2, pp. 1–60.

Chen, W.S., Huang, Y.C., Liu, C.H., Feng, H.T., Chung, S.L., Lee, Y.H., 2016. U/Pb zircon geochronology constraints on the ages of the Tananao Schist Belt and timing of orogenic events in Taiwan: implications for a new tectonic evolution of the South China Block during the Mesozoic. Tectonophysics 686, 68–81. https://doi.org/10.1016/j.tecto.2016.07.021.

Chen, W.S., Chung, S.L., Chou, H.Y., Zugeerbai, Z., Shao, W.Y., Lee, Y.H., 2017a. A reinterpretation of the metamorphic Yuli belt: evidence for a middle-late Miocene accretionary prism in eastern Taiwan. Tectonics 36 (2), 188–206. https://doi.org/10.1002/2016TC004383.

Chen, C.T., Wu, C.Y., Lo, C.H., Chu, H.T., Yui, T.F., 2017b. Dating palaeo-seismic faulting in the Taiwan Mountain Belt. Terra Nova 30, 146–151. https://doi.org/10.1111/ter.12319%.

Chiang, S.F., 2003. Original and Metamorphic P-T Evolution of Porphyroblastic Albites of Spotted Schists in Juisui, Hualien (Master). National Central University, Taoyuan.

Ching, K.E., Hsieh, M.L., Johnson, K.M., Chen, K.H., Rau, R.J., Yang, M., 2011. Modern vertical deformation rates and mountain building in Taiwan from precise leveling and continuous GPS observations, 2000-2008. J. Geophys. Res. Solid Earth 116 (B8). https://doi.org/10.1029/2011JB008242.

Chojnacki, M.R., Byrne, T.B., Ho, G.R., Lewis, J.C., Lee, J.C., Yeh, E.C., 2019. Late-stage deformation and exhumation of the blueschist-facies Yuli Belt in the Taiwan arc-continent collision. In: AGU Fall Meeting, San Francisco, California.

Clark, M.B., 1994. Kinematics and Structural Evolution of the Slate Belt and Metamorphic Core of an Active Arc-Continent Collision, Taiwan (PhD). University Park, Pennsylvania State University.

Clark, M.B., Fisher, D.M., 1995. Strain partitioning and crack-seal growth of chlorite-muscovite aggregates during progressive noncoaxial strain: an example from the Slate Belt of Taiwan. J. Struct. Geol. 17, 461–474. https://doi.org/10.1016/0191-8141(94)00071-7.

Clark, M.B., Fisher, D.M., Lu, C.Y., 1992. Strain variations in the Eocene and older rocks exposed along the central and southern cross-island highways, Taiwan. In: Science Reports of the National Taiwan University ACTA Oceanographica Taiwanica, 30, pp. 1–10.

Conand, C., Mouthereau, F., Ganne, J., Lin, A.T.S., Lahfid, A., Daudet, M., Mesalles, L., Giletycz, S., Bonzani, M., 2020. Strain partitioning and exhumation in oblique Taiwan collision: role of rift architecture and plate kinematics. Tectonics 39 (4), 1–30. https://doi.org/10.1029/2019TC005798.

Crespi, J.M., Chan, Y.C., Swaim, M.S., 1996. Synorogenic extension and exhumation of the Taiwan hinterland. Geology 24 (3), 247–250. https://doi.org/10.1130/0091-7613(1996)024<0247:SEAEOT>2.3.CO;2.

Ernst, W.G., 1983a. Mineral parageneses in metamorphic rocks exposed along Tailuko Gorge, Central Mountain Range, Taiwan. J. Metamorph. Geol. 1 (4), 305–329. https://doi.org/10.1111/j.1525-1314.1983.tb00277.x.

Ernst, W.G., 1983b. Mountain Building and Metamorphism: A Case History from Taiwan. Academic Press, London.

Ernst, W.G., Harnish, D., 1983. Mineralogy of some Tananao greenschist facies rocks, Mu-Kua Chi area, eastern Taiwan. Proc. Geol. Soc. China 26, 99–110.

Faure, M., Lu, C.Y., Chu, H.T., 1991. Ductile deformation and Miocene nappe-stacking in Taiwan related to motion of the Philippine Sea Plate. Tectonophysics 198 (1), 95–105. https://doi.org/10.1016/0040-1951(91)90134-E.

Fisher, D.M., Lu, C.Y., Chu, H.T., 2002. Taiwan Slate Belt: Insights into the Ductile Interior of an Arc-Continent Collision. Special Paper of the Geological Society of America, 358, pp. 93–106. https://doi.org/10.1130/0-8137-2358-2.93.

Fisher, D.M., Willett, S., Yeh, E.C., Clark, M.B., 2007. Cleavage fronts and fans as reflections of orogen stress and kinematics in Taiwan. Geology 35 (1), 65–68. https://doi.org/10.1130/g22850a.1.

Fuh, T.M., 1962. Metamorphic rocks of the Nanao district, Taiwan, with special reference to the origin of orthogneiss. Geol. Soc. China Mem. 1, 113–132.

Fuh, T.M., 1963. Xenoliths in an orthogneiss body of the Nanao district, Taiwan. Acta Geol. Taiwan. 11, 21–29.

Gulick, S.P., Bangs, N.L., Moore, G.F., Ashi, J., Martin, K.M., Sawyer, D.S., Tobin, H.J., Kuramoto, S.I., Taira, A., 2010. Rapid forearc basin uplift and megasplay fault development from 3D seismic images of Nankai Margin off Kii Peninsula, Japan. Earth Planet. Sci. Lett. 300 (1–2) https://doi.org/10.1016/j.epsl.2010.09.034.

Hall, R., Ali, J.R., Anderson, C.D., Baker, S.J., 1995. Origin and motion history of the Philippine Sea Plate. Tectonophysics 251 (1–4), 229–250. https://doi.org/10.1016/0040-1951(95)00038-0.

Ho, C.S., 1986. A synthesis of the geologic evolution of Taiwan. Tectonophysics 125 (1), 1–16. https://doi.org/10.1016/0040-1951(86)90004-1.

Ho, G.R., 2007. A Study of Geological Structure in the Wanrung Area, Central Range, Taiwan (Master). National Cheng Kung University, Tainan. Retrieved from. https://hdl.handle.net/11296/xw7dsz.

Ho, G.R., 2015. The Structural Evolution of the Tananao Complex, Taiwan- Taking Examples from Hopin, Wanrung and Southern Cross-Island Highway (PhD). Taipei Tech, Taipei, Taiwan. Retrieved from. https://hdl.handle.net/11296/55tpgy (95).

Ho, G.R., Lo, W., 2015. Structural analysis in Shoufengsi area of Tananao complex, Eastern Taiwan. Terr. Atmos. Ocean. Sci. 26 (5), 557–569. https://doi.org/10.3319/TAO.2015.05.15.01(TT).

Hsieh, Y.H., Liu, C.S., Suppe, J., Byrne, T.B., Lallemand, S., 2020. The Chimei submarine canyon and fan: a record of Taiwan arc-continent collision on the rapidly deforming overriding plate. Tectonics 39. https://doi.org/10.1029/2020TC006148 e2020TC006148.

Hsu, W.H., Byrne, T.B., Ouimet, W., Lee, Y.H., Chen, Y.G., Soest, M.V., Hodges, K., 2016. Pleistocene onset of rapid, punctuated exhumation in the eastern Central Range of the Taiwan orogenic belt. Geology 44 (9), 719–722. https://doi.org/10.1130/g37914.1.

Huang, C.Y., Wu, W.Y., Chang, C.P., Tsao, S., Yuan, P.B., Lin, C.W., Xia, K.Y., 1997. Tectonic evolution of accretionary prism in the arc-continent collision terrane of Taiwan. Tectonophysics 281 (1), 31–51. https://doi.org/10.1016/S0040-1951(97)00157-1.

Hwang, S.L., Yui, T.F., Chu, H.T., Shen, P., 2001. Submicron polyphase inclusions in garnet from the Tananao Metamorphic Complex, Taiwan: a key to unravelling otherwise unrecognized metamorphic events. J. Metamorph. Geol. 19 (5), 601–607. https://doi.org/10.1046/j.0263-4929.2001.00331.x.

Itoh, Y., Takemura, K., Kamata, H., 1998. History of basin formation and tectonic evolution at the termination of a large transcurrent fault system: deformation mode of central Kyushu, Japan. Tectonophysics 284 (1–2), 135–150. https://doi.org/10.1016/S0040-1951(97)00167-4.

Jahn, B.M., Liou, J.G., 1977. Age and geochemical constraints of blueschists of Taiwan. Mem. Geol. Soc. China 2, 129–140.

Jahn, B.M., Liou, J.G., Nagasawa, H., 1981. High-pressure metamorphic rocks of Taiwan: REE geochemistry, Rb–Sr ages and tectonic implications. Mem. Geol. Soc. China 4, 497–520.

Jiao, Z.H., 1991. The Geologic Structure and Evolution of the Hoping Area in Eastern Taiwan (Master). National Taiwan University, Taipei. Retrieved from. https://hdl.handle.net/11296/net82t.

Keyser, W., Tsai, C.H., Iizuka, Y., Oberhänsli, R., Ernst, W.G., 2016. High-pressure metamorphism in the Chinshuichi area, Yuli belt, eastern Taiwan. Tectonophysics 692, 191–202. https://doi.org/10.1016/j.tecto.2015.09.012.

Kisch, H.J., 1990. Calibration of the anchizone: a critical comparison of illite 'crystallinity'scales used for definition. J. Metamorph. Geol. 8 (1), 31–46.

Korren, C.S., Ferré, E.C., Yeh, E.C., Chou, Y.M., Chu, H.T., 2017. Seismic rupture parameters deduced from a Pliocene-Pleistocene fault pseudotachylyte in Taiwan. In: In, M.Y., Thomas, T.M., Bhat, Mitchell H.S. (Eds.), Fault Zone Dynamic Processes: Evolution of Fault Zone Properties and Dynamic Processes during Seismic Rupture AGU Monograph. American Geophysical Union, Washington, USA, pp. 227.

Kubler, B., 1968. Evaluation quantitative du métamorphisme par la cristallinité de l'illite. Bull. Centre Res. de Pau-SNPA 2, 385–397.

Lai, L.S.H., Dorsey, R.J., Horng, C.S., Chi, W.R., Shea, K.S., Yen, J.Y., 2021. Polygenetic mélange in the retrowedge foredeep of an active arc-continent collision, Coastal Range of eastern Taiwan. Sediment. Geol. 418, 105901. https://doi.org/10.1016/j.sedgeo.2021.105901.

Lan, C.Y., Lee, C.S., Yui, T.F., Chu, H.T., Jahn, B.M., 2008. The tectono-thermal events of Taiwan and their relationship with SE China. Terr. Atmos. Ocean. Sci. 19 (3), 257–287.

Lan, C.Y., Usuki, T., Wang, K.L., Yui, T.F., Okamoto, K., Lee, Y.H., Hirata, T., Kon, Y., Orihashi, Y., Liou, J.G., Lee, C.S., 2009. Detrital zircon evidence for the antiquity of Taiwan. Geosci. J. 13 (3), 233–243.

Lee, Y.H., Byrne, T.B., Wang, W.H., Lo, W., Rau, R.J., Lu, H.Y., 2015. Simultaneous mountain building in the Taiwan orogenic belt. Geology 43 (5). https://doi.org/10.1130/g36373.1, 451-454 %@ 0091-7613.

Lee, J.C., Ho, G.R., Byrne, T.B., Lee, Y.H., Yeh, E.C., 2019. Coeval exhumation or subduction channel extrusion of the high pressure Yuli belt? Insights from the Shoufeng fault in eastern Taiwan. In: JpGU Meeting, Chiba, Japan.
Lin, M.L., 1986. Petrotectonic Study on the Yuli Belt of Tananao Schist in the Chinshuichi Area, Yuli, Hualien, Taiwan (PhD). National Taiwan University, Taipei. Retrieved from. https://hdl.handle.net/11296/ua639x.
Lin, M.L., Yang, C.N., Wang, Y., 1984. Petrotectonic study on the Yuli belt of the Tananao Schist in the Chinshuichi area, eastern Taiwan. In: Science Reports of the National Taiwan University ACTA Geologica Taiwanica, 22, pp. 151–188.
Liou, J.G., 1981. Petrology of metamorphosed oceanic rocks in the Central Range of Taiwan. Mem. Geol. Soc. China 4, 291–342.
Liou, J.G., Ho, C.O., Yen, T.P., 1975. Petrology of some Glaucophane Schists and related rocks from Taiwan. J. Petrol. 16 (1), 80–109. https://doi.org/10.1093/petrology/16.1.80.
Lo, C.H., Onstott, T.C., 1995. Rejuvenation of KAr systems for minerals in the Taiwan Mountain Belt. Earth Planet. Sci. Lett. 131 (1), 71–98. https://doi.org/10.1016/0012-821X(95)00011-Z.
Lo, C.H., Yui, T.F., 1996. $^{40}Ar/^{39}Ar$ dating of high-pressure rocks in the Tananao basement complex, Taiwan. J. Geol. Soc. China 39, 13–130.
Lu, C.Y., Hsu, K.J., 1992. Tectonic evolution of the Taiwan mountain belt. Pet. Geol. Taiwan 27, 21–46.
Lu, C.Y., Wang Lee, C.M., 1986. The sheath folds in the Tananao Group between Tienshiang and Tailuko, east-west cross-island highway, Taiwan. Tectonophysics 125 (1), 125–131. https://doi.org/10.1016/0040-1951(86)90010-7.
Lu, C.Y., Chang, K.J., Malavieille, J., Chan, Y.C., Chang, C.P., Lee, J.C., 2001. Structural evolution of the southeastern Central Range, Taiwan. W. Pac. Earth Sci. 1 (2), 213–226.
Malavieille, J., Dominguez, S., Lu, C.Y., Chen, C.T., Konstantinovskaya, E., 2019. Deformation partitioning in mountain belts: insights from analogue modelling experiments and the Taiwan collisional orogen. Geol. Mag. 158 (1), 84–103. https://doi.org/10.1017/S0016756819000645.
Merriman, R.J., Frey, M., 1999. Patterns of Very Low-Grade Metamorphism in Metapelitic Rocks. Blackwell Science.
Mesalles, L., 2014. Mountain Building at a Subduction-Collision Transition Zone, Taiwan: Insights from Morphostructural Analysis and Thermochronological Dating (PhD). Université Pierre et Marie Curie - Paris VI, 336.
Mesalles, L., Mouthereau, F., Bernet, M., Chang, C.P., Lin, T.S.A., Fillon, C., Sengelen, X., 2014. From submarine continental accretion to arc-continent orogenic evolution: the thermal record in southern Taiwan. Geology 42 (10), 907–910. https://doi.org/10.1130/G35854.1.
Mizuno, K., Tsukuda, E., Takahashi, M., Momohara, A., Uchiyama, T., 1999. Subsurface geology of the Wakayama Plain, southwestern Japan based on the deep boring survey. J. Geol. Soc. Jpn. 105 (3), 235–238.
Mondro, C.A., Fisher, D., Yeh, E.C., 2017. Strain histories from the eastern Central Range of Taiwan: a record of advection through a collisional orogen. Tectonophysics 705, 1–11. https://doi.org/10.1016/j.tecto.2017.03.007.
Mouthereau, F., Conand, C., Larrey, M., 2019. Strain partitioning of oblique convergence and role of rift inheritance in orogens. In: AGU Fall Meeting, San Francisco, California.
Nakamura, K., Renard, V., Angelier, J., Azema, J., Bourgois, J., Deplus, C., Fujioka, K., Hamano, Y., Huchon, P., Kinoshita, H., Labaume, P., Ogawa, Y., Seno, T., Takeuchi, A., Tanahashi, M., Uchiyama, A., Vigneresse, J.L., 1987. Oblique and near collision subduction, Sagami and Suruga Troughs—preliminary results of the French-Japanese 1984 Kaiko cruise, Leg 2. Earth Planet. Sci. Lett. 83 (1–4), 229–242. https://doi.org/10.1016/0012-821X(87)90068-9.
Page, B., Suppe, J., 1981. The Pliocene Lichi Melange of Taiwan: its plate-tectonic and olistostromal origin. Am. J. Sci. 281, 193–227. https://doi.org/10.2475/ajs.281.3.193.
Panozzo, R., 1987. Two-dimensional strain determination by the inverse Surfor wheel. J. Struct. Geol. 9 (1), 115–119. https://doi.org/10.1016/0191-8141(87)90049-6.
Pelletier, B., Stephan, J.F., 1986. Middle Miocene obduction and Late Miocene Beginning of collision registered in the Hengchun peninsula: geodynamic implications for the evolution of Taiwan. Mem. Geol. Soc. China 7, 301–324.
Pulver, M.H., Crespi, J.M., Byrne, T.B., 2002. Lateral extrusion in a transpressional collision zone: an example from the pre-Tertiary metamorphic basement of Taiwan. Geol. Soc. Am. Spec. Pap. 358, 107–120.
Rau, R.J., Ching, K.E., Hu, J.C., Lee, J.C., 2008. Crustal deformation and block kinematics in transition from collision to subduction: global positioning system measurements in northern Taiwan, 1995–2005. J. Geophys. Res. Solid Earth 113 (B9). https://doi.org/10.1029/2007JB005414.
Sacks, A., Saffer, D.M., Fisher, D., 2013. Analysis of normal fault populations in the Kumano forearc basin, Nankai Trough, Japan: 2. Principal axes of stress and strain from inversion of fault orientations. Geochem. Geophys. Geosyst. 14 (6), 1973–1988.
Sandmann, S., Nagel, T.J., Froitzheim, N., Ustaszewski, K., Münker, C., 2015. Late Miocene to Early Pliocene blueschist from Taiwan and its exhumation via forearc extraction. Terra Nova 27 (4), 285–291. https://doi.org/10.1111/ter.12158.
Sato, H., Kato, N., Abe, S., Van Horne, A., Takeda, T., 2015. Reactivation of an old plate interface as a strike-slip fault in a slip-partitioned system: median Tectonic Line, SW Japan. Tectonophysics 644, 58–67. https://doi.org/10.1016/j.tecto.2014.12.020.
Sibuet, J.C., Letouzy, J., Barbier, F., Charvet, J., Foucher, J.P., Hilde, T.W.C., Kimura, M., Lin-Yun, C., Marsset, B., Muller, C., Stephan, J.F., 1987. Back arc extension in the Okinawa Trough. J. Geophys. Res. 92 (B13), 14041–14063. https://doi.org/10.1029/JB092iB13p14041.
Stanley, R.S., Hill, L.B., Chang, H.C., Hu, H.N., 1981. A transect through the metamorphic core of the Central Mountains, southern Taiwan. Mem. Geol. Soc. China 4, 443–473.
Stipp, M., Stünitz, H., Heilbronner, R., Schmid, S.M., 2002. The eastern Tonale fault zone: a 'natural laboratory' for crystal plastic deformation of quartz over a temperature range from 250 to 700°C. J. Struct. Geol. 24 (12), 1861–1884. https://doi.org/10.1016/S0191-8141(02)00035-4.
Sung, Q., 1991. The Geological Sheet Map Hengchun Peninsula, Scale 1:50,000, and Its Explanatory Text. Central Geological Survey, MOEA.
Suppe, J., 1984. Kinematics of arc-continent collision, flipping of subduction, and back-arc spreading near Taiwan. Mem. Geol. Soc. China 6, 21–33. Retrieved from. https://ci.nii.ac.jp/naid/10017470069/en/.
Teng, L.S., 1996. Extensional collapse of the northern Taiwan mountain belt. Geology 24 (10), 949–952. https://doi.org/10.1130/0091-7613(1996)024<0949:Ecotnt>2.3.Co;2.
Tillman, K.S., Byrne, T.B., 1995. Kinematic analysis of the Taiwan Slate Belt. Tectonics 14 (2), 322–341. https://doi.org/10.1029/94TC02451.
Tsai, C.H., Iizuka, Y., Ernst, W.G., 2013. Diverse mineral compositions, textures, and metamorphic P-T conditions of the glaucophane-bearing rocks in the Tamayen mélange, Yuli belt, eastern Taiwan. J. Asian Earth Sci. 63, 218–233. https://doi.org/10.1016/j.jseaes.2012.09.019.
Tsao, S.J., 1996. The Geological Significances of Illite Crystallinity, Zircon Fission-Track Ages, and K-Ar Ages of Metasedimentary Rocks of the Central Range of Taiwan (PhD). National Taiwan University, Taipei. Retrieved from. https://hdl.handle.net/11296/aykz26.
Tsao, S.J., Li, T.C., Tien, R.L., Chen, C.H., Liu, T.K., Chen, C.H., 1992. Illite crystallinity and fission-track ages along the east central cross-island highway of Taiwan. In: Science Reports of the National Taiwan University ACTA Geologica Taiwanica, 30, pp. 45–64.
Tsutsumi, Y., Yokoyama, K., Shen, J.J.S., Horie, K., Terada, K., Hidaka, H., Lee, C.S., 2011. SHRIMP U–Pb zircon geochronology of the orthogneiss and paragneiss in the Eastern Central Range, Taiwan. Bull. Natl. Mus. Nat. Sci. Ser. C 37, 17–27.
Verdel, C., Niemi, N., Van der Pluijm, B.A., 2011. Variations in the illite to muscovite transition related to metamorphic conditions and detrital muscovite content: insight from the paleozoic passive margin of the southwestern United States. J. Geol. 119 (4), 419–437. https://doi.org/10.1086/660086%U.
Wang Lee, C., Wang, Y., Yen, T.P., Lo, C.H., 1982. Polymetamorphism in some gneiss bodies, Hoping-Chipan area, Hualien, eastern Taiwan. Acta Geol. Taiwan. 21, 122–139.
Wang, Y., Yang, C.N., 1979. Evidences for polymetamorphism and multiple deformation in the Tananao Schist. Ti-Chih 2, 39–45.
Wang, P.L., Lin, L.H., Lo, C.H., 1998. $^{40}Ar/^{39}Ar$ dating of mylonitization in the Tananao schist, eastern Taiwan. J. Geol. Soc. China 41 (2), 159–183.
Warneke, L.A., Ernst, W.G., 1984. Progressive Cenozoic metamorphism of rocks cropping out along the southern east-west cross-island highway, Taiwan. Mem. Geol. Soc. China 6, 105–132.
Willett, S.D., Fisher, D., Fuller, C., Yeh, E.C., Lu, C.Y., 2003. Erosion rates and orogenic-wedge kinematics in Taiwan inferred from fission-track thermochronometry. Geology 11, 945–948. https://doi.org/10.1130/g19702.1.
Wu, J., Suppe, J., Lu, R., Kanda, R., 2016. Philippine Sea and East Asian plate tectonics since 52Ma constrained by new subducted slab reconstruction methods. J. Geophys. Res. Solid Earth 121 (6), 4670–4741. https://doi.org/10.1002/2016JB012923.
Yamaji, A., 2000. The multiple inverse method applied to meso-scale faults in mid-Quaternary fore-arc sediments near the triple trench junction off central Japan. J. Struct. Geol. 22 (4), 429–440. https://doi.org/10.1016/S0191-8141(99)00162-5.
Yeh, E.C., 1998. The Ductile Shear Deformation and Structural Evolution of the Penglai Orogeny at Suao-Donao Area in Northeastern Taiwan (Master). National Taiwan University, Taipei. Retrieved from. https://hdl.handle.net/11296/fq8qpk.
Yeh, E.C., Wu, Y.M., Shyu, J.B.H., Chang, C.H., 2016. Tectonic implication of the 5th March 2005, doublet earthquake in Ilan, Taiwan. Terr. Atmos. Ocean. Sci. 27, 799–805. https://doi.org/10.3319/TAO.2016.02.26.01(T).
Yen, T.P., 1953. On the occurrence of the late Paleozoic fossils in the metamorphic complex of Taiwan. Bull. Geol. Surv. Taiwan 4, 23–26.
Yen, T.P., 1960. A stratigraphical study on the Tananao Schist in Northern Taiwan. Bull. Geol. Surv. Taiwan 12, 53–66.
Yen, T.P., 1963. The metamorphic belts within the Tananao Schist terrain of Taiwan. Proc. Geol. Soc. China 6, 72–74.
Yen, T.P., 1967. Structural analysis of the Tananao Schist of Taiwan. Bull. Geol. Surv. Taiwan 18, 1–110.
Yen, T.P., Sheng, C.C., Keng, W.P., 1951. The Discovery of fusuline limestone in the metamorphic complex of Taiwan. Bull. Geol. Surv. Taiwan 3, 23–25.
Yi, T.C., Chen, Z.Y., Lin, C.W., 2012. The Geological Sheet Map "Guangfu", Scale 1: 50,000, and Its Explanatory Text. Central Geological Survey, MOEA, New Taipei city, Taiwan.
Yui, T.F., 2005. Isotopic composition of carbonaceous material in metamorphic rocks from the mountain belt of Taiwan. Int. Geol. Rev. 47 (3), 310–325. https://doi.org/10.2747/0020-6814.47.3.310.
Yui, T.F., Jeng, R.C., 1990. A stable isotope study of the hydrothermal alteration of the East Taiwan Ophiolite. Chem. Geol. 89, 65–85.
Yui, T.F., Lo, C.H., 1989. High-pressure metamorphosed ophiolitic rocks from the Wanjung area, Taiwan. Proc. Geol. Soc. China 32 (1), 47–62.
Yui, T.F., Huang, E., Xu, J., 1996. Raman spectrum of carbonaceous material: a possible metamorphic grade indicator for low-grade metamorphic rocks. J. Metamorph. Geol. 14 (2), 115–124. https://doi.org/10.1046/j.1525-1314.1996.05792.x.
Yui, T.F., Okamoto, K., Usuki, T., Lan, C.Y., Chu, H.T., Liou, J.G., 2009. Late Triassic–Late Cretaceous accretion/subduction in the Taiwan region along the eastern margin of South China – evidence from zircon SHRIMP dating. Int. Geol. Rev. 51 (4), 304–328. https://doi.org/10.1080/00206810802636369.

Yui, T.F., Maki, K., Lan, C.Y., Hirata, T., Chu, H.T., Kon, Y., Yokoyama, T.D., Jahn, B.M., Ernst, W.G., 2012. Detrital zircons from the Tananao metamorphic complex of Taiwan: Implications for sediment provenance and Mesozoic tectonics. Tectonophysics 541-543, 31–42. https://doi.org/10.1016/j.tecto.2012.03.013.

Yui, T.F., Usuki, T., Chen, C.Y., Ishida, A., Sano, Y., Suga, K., Iizuka, Y., Chen, C.T., 2014. Dating thin zircon rims by NanoSIMS: the Fengtien nephrite (Taiwan) is the youngest jade on Earth. Int. Geol. Rev. 56 (16), 1932–1944. https://doi.org/10.1080/00206814.2014.972994.

Zhang, Y., Tsai, C.H., Froitzheim, N., Ustaszewski, K., 2020. The Yuli Belt in Taiwan: part of the suture zone separating Eurasian and Philippine Sea plates. Terr. Atmos. Ocean. Sci. 31 (4), 415–435. https://doi.org/10.3319/TAO.2020.06.28.01.